NASA Technical Memorandum 83171

Stability and Control Characteristics of a Three-Surface Advanced Fighter Configuration at Angles of Attack up to 45°

William P. Henderson and Laurence D. Leavitt

SEPTEMBER 1981

NASA

NASA Technical Memorandum 83171

Stability and Control Characteristics of a Three-Surface Advanced Fighter Configuration at Angles of Attack up to 45°

William P. Henderson and Laurence D. Leavitt
Langley Research Center
Hampton, Virginia

National Aeronautics
and Space Administration

**Scientific and Technical
Information Branch**

1981

SUMMARY

An investigation has been conducted to determine the stability and control characteristics of a three-surface (canard-wing-horizontal-tail) advanced fighter configuration. The tests were conducted at Mach numbers from 0.40 to 0.90, at angles of attack up to 45° for the lower Mach numbers, and at angles of sideslip up to 15°. The model variations under study included adding a canard surface and deflecting horizontal tails, ailerons, and rudders. Adding the canard results in a favorable interaction with the wing which keeps the flow attached at higher angles of attack and increases the maximum lift coefficient obtained. The 20° dihedral canard, because of its small size and proximity to the wing and moment reference center, provides small levels of pitch trim moment and essentially no roll control. The horizontal tails are quite effective in producing both trim moment and roll control at the higher angles of attack. At an angle of attack of 31°, the canard caused a significant nonlinearity in the variation of the rolling-moment coefficient with sideslip angle at sideslip angles between ±5.0°. This rolling-moment nonlinearity can be eliminated by addition of a fuselage forebody strake or by combined deflection of the canard and horizontal tails.

INTRODUCTION

Future fighter aircraft may be required to perform in many different flight regimes. For example, a fighter designed for efficient cruise may be required to operate over a large angle of attack range, even at angles of attack beyond wing stall. To achieve this truly multimission capability, new technologies such as thrust vectoring, thrust reversing, vortex flow control, and favorable canard-wing interaction must be considered in the design of fighter aircraft. As a result, NASA has devoted considerable research effort to developing these technologies for application to the next generation of fighter aircraft (see ref. 1). Thrust vectoring and reversing on high performance aircraft configurations have received considerable attention in the past several years and have been shown to provide improved maneuverability and shorter take-off and landing distances (see ref. 2). Taking full advantage of thrust vectoring technology will probably require incorporation of an auxiliary trimming device such as a canard surface. This canard, mounted ahead of the wing, can provide the needed control forces as well as favorable canard-wing interactions at high angles of attack (see ref. 3). Limited research has been conducted, primarily on simplified configurations, to determine the interactions associated with the addition of the canard. However, little research into these interactions has been done on realistic fighter-type configurations. It is the purpose of this paper to present the results of a study to determine the high angle of attack characteristics of a high performance fighter aircraft with a canard surface incorporated. The study was conducted in the Langley 16-Foot Transonic Tunnel at Mach numbers up to 0.90, angles of attack up to 45°, and angles of sideslip up to 15°.

SYMBOLS

All longitudinal forces and moments are referred to the wind axis system, and the lateral-directional forces and moments are referred to the body axis system. All data are presented with respect to a center-of-gravity position of 25.65 percent of the wing mean geometric chord (see fig. 1). Dimensional quantities are presented in both SI and U.S. Customary Units. The measurements and calculations were made in U.S. Customary Units.

b wing span, m (ft)

C_D drag coefficient, $\frac{\text{Drag}}{qS}$

C_L lift coefficient, $\frac{\text{Lift}}{qS}$

C_l rolling-moment coefficient, $\frac{\text{Rolling moment}}{qSb}$

C_m pitching-moment coefficient, $\frac{\text{Pitching moment}}{qS\bar{c}}$

C_n yawing-moment coefficient, $\frac{\text{Yawing moment}}{qSb}$

C_Y side-force coefficient, $\frac{\text{Side force}}{qS}$

$\bar{c}$ mean geometric chord, m (ft)

M free-stream Mach number

q free-stream dynamic pressure, Pa (lb/ft^2)

S wing reference area, m^2 (ft^2)

α angle of attack, deg

β angle of sideslip, deg

δ_a aileron deflection angle (positive when trailing edge is down), deg

δ_c canard deflection angle (positive when leading edge is up), deg

δ_h horizontal tail deflection angle (positive when leading edge is up), deg

δ_r rudder deflection angle (positive when trailing edge is left), deg

Γ_c canard dihedral angle (positive when tip is up), deg

Subscripts:

L left

R right

MODEL

The investigation was conducted using a 0.047-scale model of an advanced fighter concept modified to include an all-movable canard mounted on the inlet. A three-view sketch of the model is shown in figure 1. A forebody strake whose size and location were determined from experimental tests made in the Langley 12-Foot Low-Speed Tunnel (see ref. 4) is shown mounted on the configuration in figure 1. (This strake was added to improve flow characteristics over the forebody.) Photographs of the model are presented in figure 2, and geometric characteristics are presented in table I.

TEST AND CORRECTIONS

The investigation was conducted in the Langley 16-Foot Transonic Tunnel at Mach numbers from 0.40 to 0.90, at angles of attack from -5° to 45°, and at sideslip angles from -5° to 15°. The variation of test Reynolds number based on the wing mean geometric chord is presented in the following table:

M	Reynolds number
0.40	1.90×10^6
.60	2.45
.90	2.98

Boundary layer transition strips (0.32 cm (1/8 in.) wide) of No. 120 carborundum grains (sized on the basis of criteria in ref. 5) were placed 1.27 cm (1/2 in.) behind the leading edge of the wings, canard, and tail surfaces and 2.54 cm (1 in.) behind the nose of the fuselage.

Aerodynamic forces and moments were measured by an internal six-component strain-gage balance. Model angle of attack was obtained by correcting the angle of the model support system for deflection of the sting and balance under aerodynamic loads and for test-section stream angularity. The force data are adjusted to the conditions of free-stream static pressure at the fuselage base. Internal drag values obtained from unpublished data supplied by McDonnell-Douglas Corp., resulting from flow through the model, inlet, and exhaust system, were subtracted from the model total drag coefficient. The values of internal drag are listed in table II.

PRESENTATION OF RESULTS

The results of this investigation are presented in the figures as follows:

RESULTS AND DISCUSSION

The major emphasis in this program was the study of the stability and control characteristics of a three-surface (canard-wing-horizontal-tail) configuration at high angles of attack. The longitudinal aerodynamic characteristics of the configuration are presented in figure 3. The basic configuration without the canard produced a maximum lift coefficient less than 1.60 and an early break in the lift curve (probably at an angle of attack less than 15°) which indicates flow separation on the wing. Adding the canard resulted in a favorable interaction with the wing, as has been shown in previous studies (for example, refs. 6 and 7). This interaction kept the flow attached at higher angles of attack and increased the maximum lift coefficient. While all of the longitudinal aerodynamic data were obtained with a canard dihedral angle of 20°, some effects of canard dihedral are presented for the lateral-directional characteristics. Data presented in reference 8 indicate that the highest value of maximum lift coefficient is obtained for a configuration with the canard and wing root chords in the same plane, provided that the canard was positioned at a positive dihedral angle. The present three-surface configuration, therefore, should exhibit improved maneuvering characteristics at higher angles of attack providing that the canard does not cause a deterioration in the stability and control characteristics.

The canard, because of its small size and proximity to the wing and moment reference center, provides only small levels of pitch trim moment (see fig. 4) at angles of attack below 40° and essentially no roll control (fig. 7(b)). Differential deflection of the canard does provide some side force (fig. 7(b)) at the higher angles of attack. While there are insufficient data to determine the mechanism for producing this side force, previous studies have indicated that these effects are caused by interference pressures on the fuselage in the vicinity of the canard. Horizontal tails are very effective in producing both pitch trim moment (fig. 5) and roll control (see fig. 9(b)) at these higher angles of attack. Note that differential deflection of the horizontal tails also produces adverse yawing moment above an angle of attack of 27°. The rudders are effective in producing yawing moment (see fig. 6(b)) at angles of attack up to at least 40°, and deflection of the ailerons produces roll control (see fig. 8(b)), with only a slight adverse yawing moment.

The effects of angle of attack on the lateral-directional characteristics as a function of sideslip angle for the various configuration modifications are presented in figures 10 through 13. These data indicate a reduction in the directional stability of the configuration as angle of attack is increased. This is probably because of a loss in vertical tail effectiveness caused by adverse fuselage flow-field effects. The data of figures 10 through 13 are replotted in figures 14 through 16 so that the effects of the modifications can be easily seen. At an angle of attack of 21° (see fig. 14(a)), adding the canard and strake does not significantly alter the linearity of the data but does produce a destabilizing increment in the directional stability C_{n_β}. This effect should be expected since the canard and strake alter the flow around the fuselage forebody. At an angle of attack of 31° (see fig. 14(b)), the canard caused a significant nonlinearity in the variation of the rolling-moment coefficient with sideslip angle at sideslip angles between ±5.0°. The cause of this nonlinearity is not fully understood, but it is believed to be associated

with the asymmetrical shedding of vortexes off the forebody which affect the wing flow field. Note the indication of flow separation on the canard at angles of attack around 30°, as illustrated by the break in the lift curve and pitching moment shown in figure 3. Adding the forebody strake alters these flow characteristics so that the rolling-moment nonlinearity between sideslip angles of ±5.0° is eliminated. At an angle of attack of 46° (see fig. 14(c)), the flow again appears to be stabilized so that installation of the canard has little or no effect on the rolling-moment coefficient below a sideslip angle of 8°.

The effect of angle of attack on the lateral-directional characteristics for the configuration with combined canard and horizontal tail deflections is presented in figure 17 and replotted in figure 18 to show the effects of control surface deflection at a given angle of attack. Note that the nonlinearity in rolling-moment coefficient which occurs at low angles of sideslip has moved to higher sideslip angles (above 8°) when the horizontal tails are deflected -25° and is essentially eliminated when the canard is also deflected to -27°. Unloading the canard has eliminated the vortex flow off the forebody.

SUMMARY OF RESULTS

A study has been conducted to determine the stability and control characteristics of a three-surface (canard-wing-horizontal-tail) fighter-type configuration at angles of attack up to 45°. As a result of this study, the following conclusions can be drawn:

1. Adding the canard results in a favorable interaction with the wing which keeps the flow attached at higher angles of attack and increases the maximum lift coefficient obtained.

2. The 20° dihedral canard, because of its small size and proximity to the wing and the center of gravity, provides small levels of pitch trim moment and essentially no roll control.

3. The horizontal tails are quite effective in producing both pitch trim moment and roll control at the higher angles of attack.

4. At an angle of attack of 31°, the canard caused a significant nonlinearity in the variation of the rolling-moment coefficient with sideslip angle at sideslip angles between ±5.0°. This rolling-moment nonlinearity was eliminated by adding a fuselage forebody strake or by combined deflection of the canard and horizontal tails.

Langley Research Center
National Aeronautics and Space Administration
Hampton, VA 23665
August 3, 1981

REFERENCES

1. Tactical Aircraft Research and Technology - Volume I. NASA CP-2162, 1981.

2. Capone, Francis J.: The Nonaxisymmetric Nozzle - It is for Real. AIAA Paper 79-1810, Aug. 1979.

3. Gloss, Blair B.; and McKinney, Linwood W.: Canard-Wing Lift Interference Related to Maneuvering Aircraft at Subsonic Speeds. NASA TM X-2897, 1973.

4. Agnew, J. W.; Lyerla, G. W.; and Grafton, S. B.: The Linear and Non-Linear Aerodynamics of Three-Surface Aircraft Concepts. A Collection of Technical Papers - AIAA Atmospheric Flight Mechanics Conference, Aug. 1980, pp. 211-221. (Available as AIAA-80-1581.)

5. Braslow, Albert L.; Hicks, Raymond M.; and Harris, Roy V., Jr.: Use of Grit-Type Boundary-Layer-Transition Trips on Wind-Tunnel Models. NASA TN D-3579, 1966.

6. Henderson, William P.: The Effect of Canard and Vertical Tails on the Aerodynamic Characteristics of a Model With a 59° Sweptback Wing at a Mach Number of 0.30. NASA TM X-3088, 1974.

7. Gloss, Blair B.: Effect of Wing Planform and Canard Location and Geometry on the Longitudinal Aerodynamic Characteristics of a Close-Coupled Canard Wing Model at Subsonic Speeds. NASA TN D-7910, 1975.

8. Gloss, Blair B.: The Effect of Canard Leading-Edge Sweep and Dihedral Angle on the Longitudinal and Lateral Aerodynamic Characteristics of a Close-Coupled Canard-Wing Configuration. NASA TN D-7814, 1974.

TABLE I.- MODEL GEOMETRIC CHARACTERISTICS

Overall model length, m (ft)	0.93 (3.05)
Wing:	
Span, m (ft)	0.612 (2.007)
Area, m^2 (ft^2)	0.124 (1.34)
Root chord (theoretical), m (ft)	0.33 (1.07)
Tip chord (theoretical), m (ft)	0.082 (0.27)
Mean geometric chord, m (ft)	0.228 (0.749)
Aspect ratio	3.0
Taper ratio	0.25
Sweepback of leading edge, deg	45
Airfoil section	NACA 64A series[a]
Horizontal tail (exposed each side):	
Span, m (ft)	0.113 (0.37)
Area, m^2 (ft^2)	0.012 (0.133)
Root chord (theoretical), m (ft)	0.165 (0.54)
Tip chord (theoretical), m (ft)	0.055 (0.18)
Sweepback of leading edge, deg	50
Airfoil section	NACA 64-series
Vertical tail (exposed each panel):	
Span, m (ft)	0.146 (0.48)
Area, m^2 (ft^2)	0.013 (0.138)
Root chord, m (ft)	0.137 (0.45)
Tip chord, m (ft)	0.037 (0.12)
Sweepback of leading edge, deg	36.57
Toe-out angle, deg	2
Airfoil section	NACA 64-series
Rudder:	
Span, m (ft)	0.067 (0.22)
Hinge-line location, percent chord	71
Canard (exposed each panel):	
Span, m (ft)	0.088 (0.29)
Area, m^2 (ft^2)	0.006 (0.066)
Root chord, m (ft)	0.113 (0.37)
Tip chord, m (ft)	0.028 (0.092)
Sweepback of leading edge, deg	50
Airfoil section	NACA 64-series
Aileron:	
Inboard chord, m (ft)	0.043 (0.14)
Outboard chord, m (ft)	0.027 (0.09)
Span, m (ft)	0.076 (0.25)

[a]Airfoil section has conical camber of design $C_L = 0.3$ on the outboard 20 percent of the local semispan.

TABLE II.- INTERNAL DRAG CHARACTERISTICS

α, deg	$C_{D,i}$ for -		
	M = 0.40	M = 0.60	M = 0.90
-6.0	0.00338	0.00338	0.00416
-4.0	.00231	.00231	.00276
-2.0	.00140	.00140	.00163
0	.00090	.00090	.00109
2.0	.00070	.00070	.00090
4.0	.00071	.00071	.00089
6.0	.00078	.00078	.00091
8.0	.00087	.00087	.00095
10.0	.00100	.00100	.00101
15.0	.00135	.00135	.00118
20.0	.00164	.00164	.00135
25.0	.00196	.00196	.00150
30.0	.00219		
35.0	.00242		
40.0	.00259		
45.0	.00268		

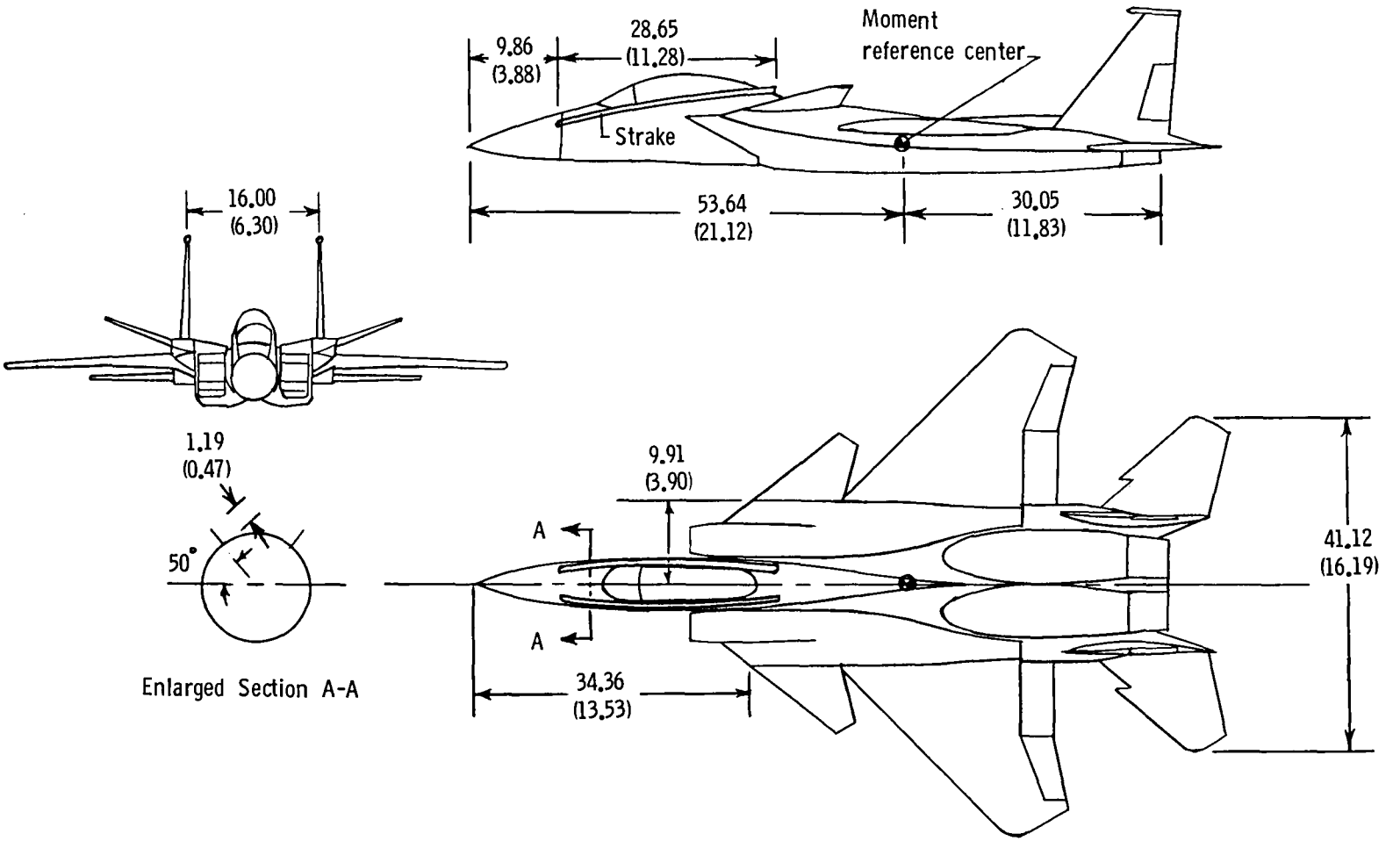

Figure 1.- Three-view drawing of configuration. (All dimensions are in centimeters (inches) unless noted.)

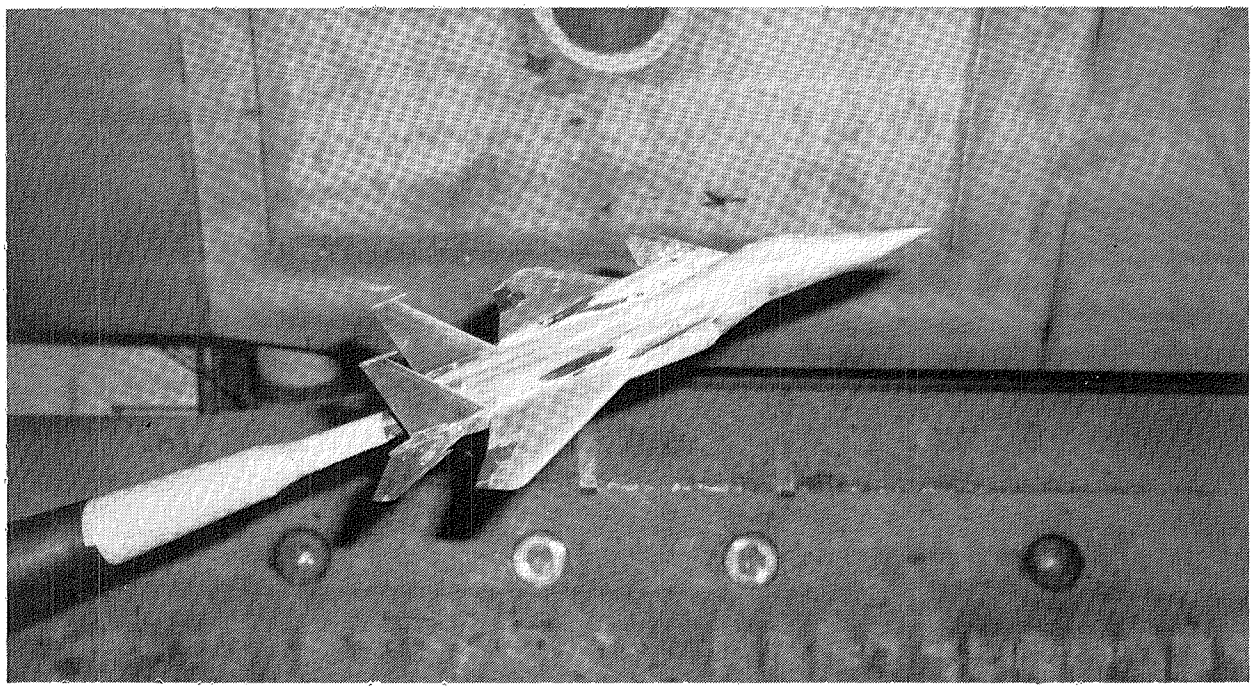

L-80-3422

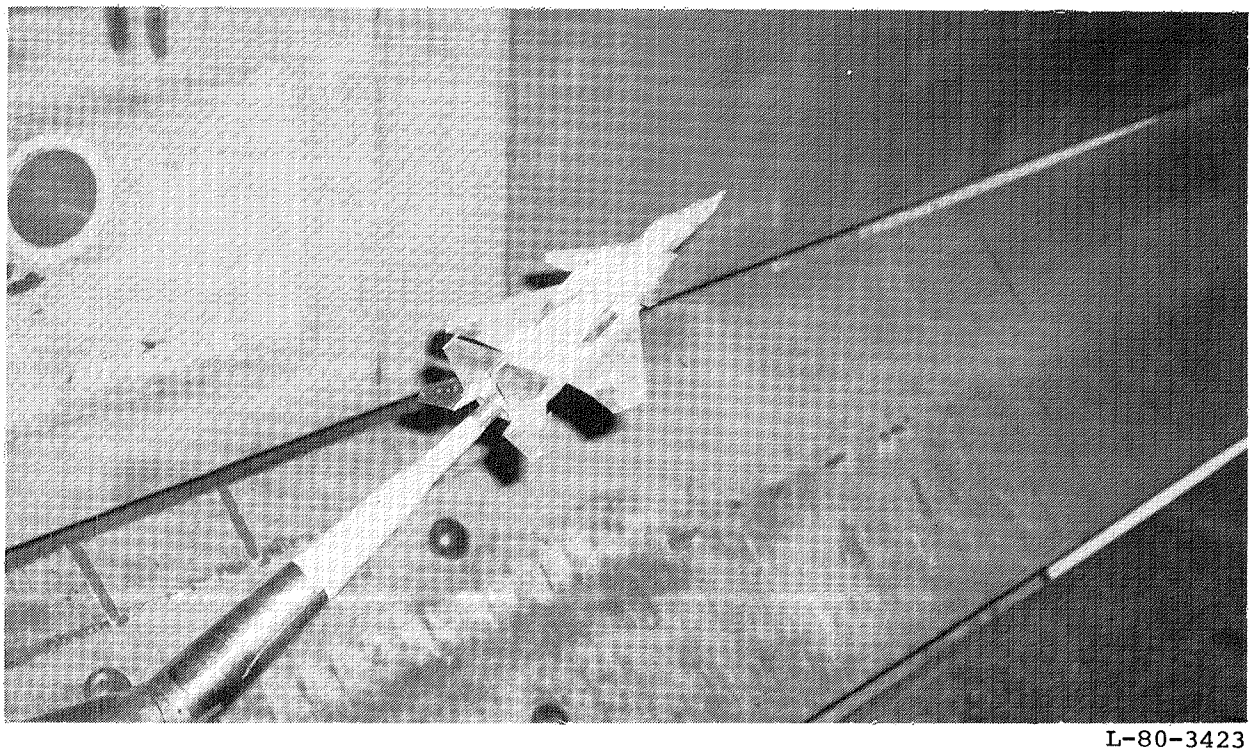

L-80-3423

Figure 2.- Photographs of model in Langley 16-Foot Transonic Tunnel.

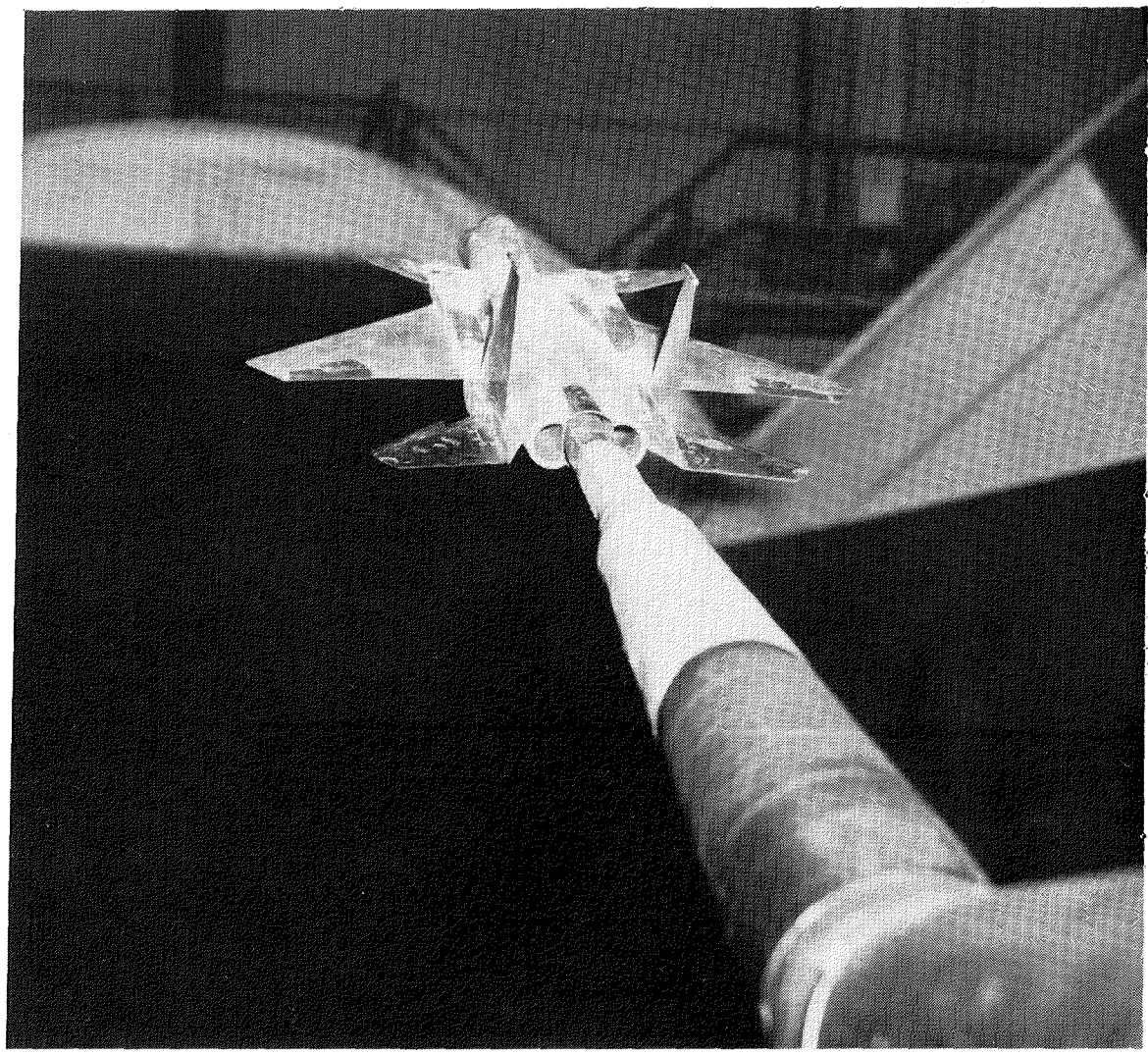

L-80-3421

Figure 2.- Concluded.

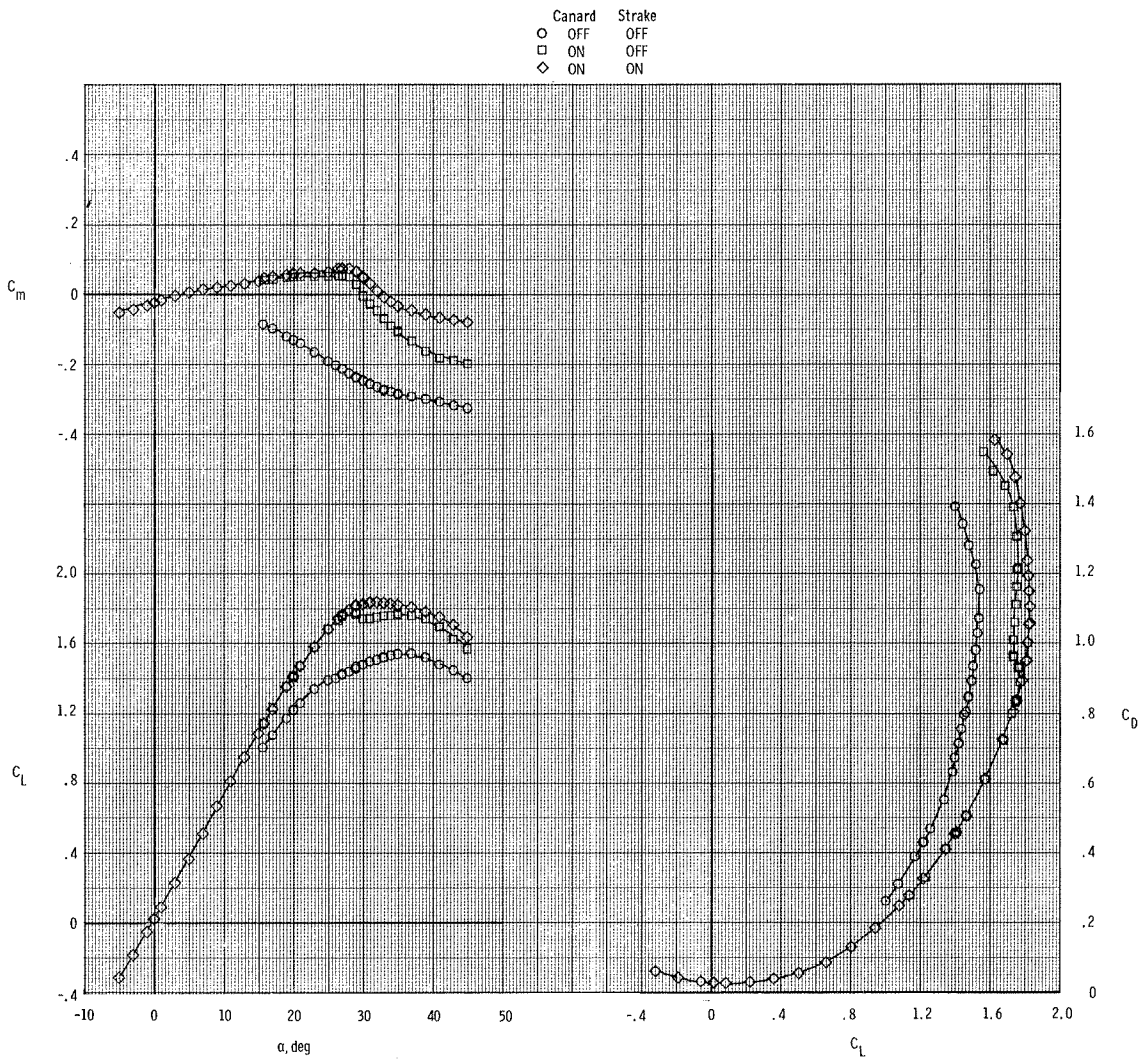

Figure 3.- Effect of canard and strake on longitudinal aerodynamic characteristics. M = 0.40; Γ_c = 20°; δ_c = -9°; δ_h = 0°.

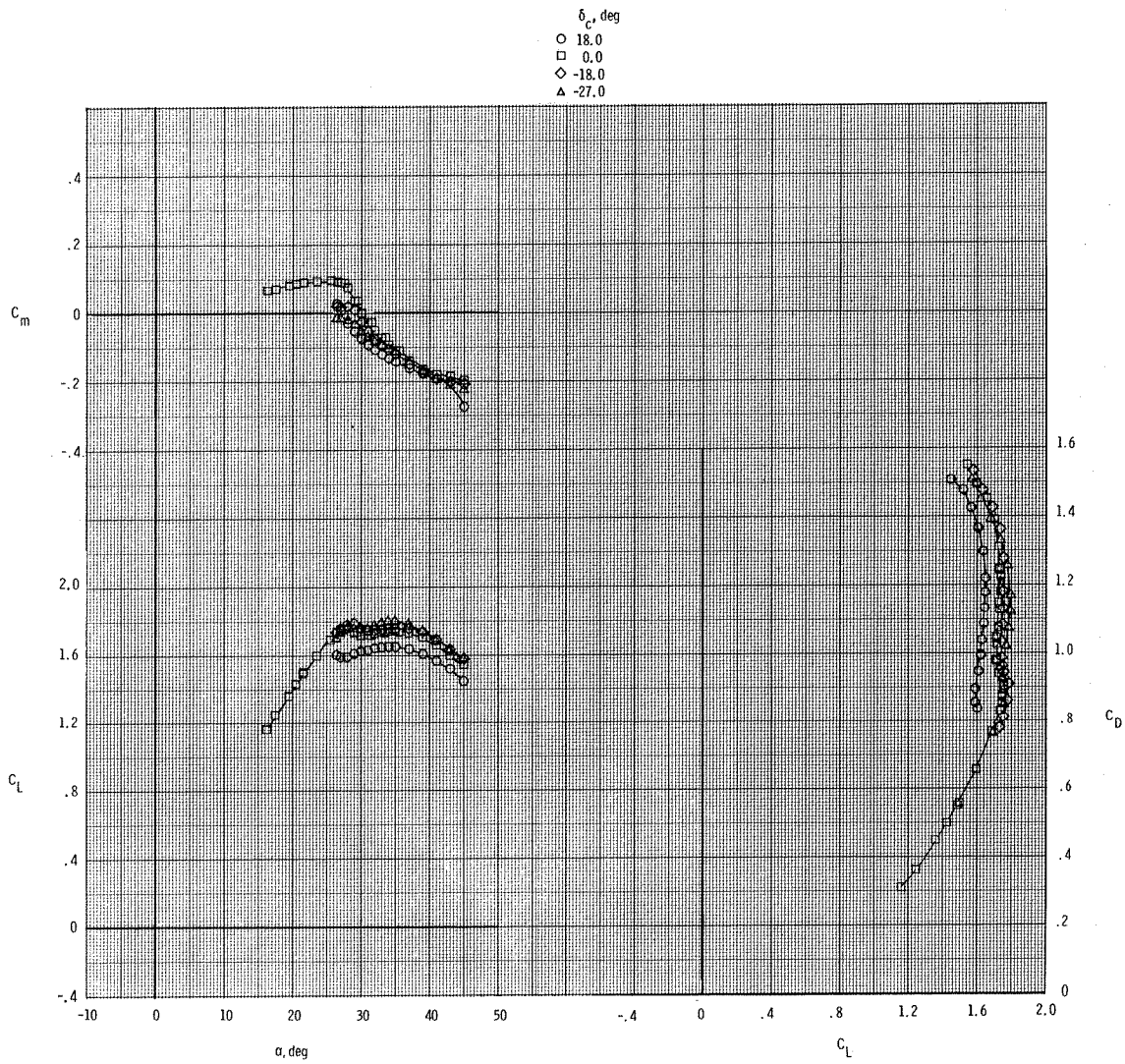

Figure 4.- Effect of canard deflection on the longitudinal aerodynamic characteristics. M = 0.40; Γ_c = 20°; δ_h = 0°.

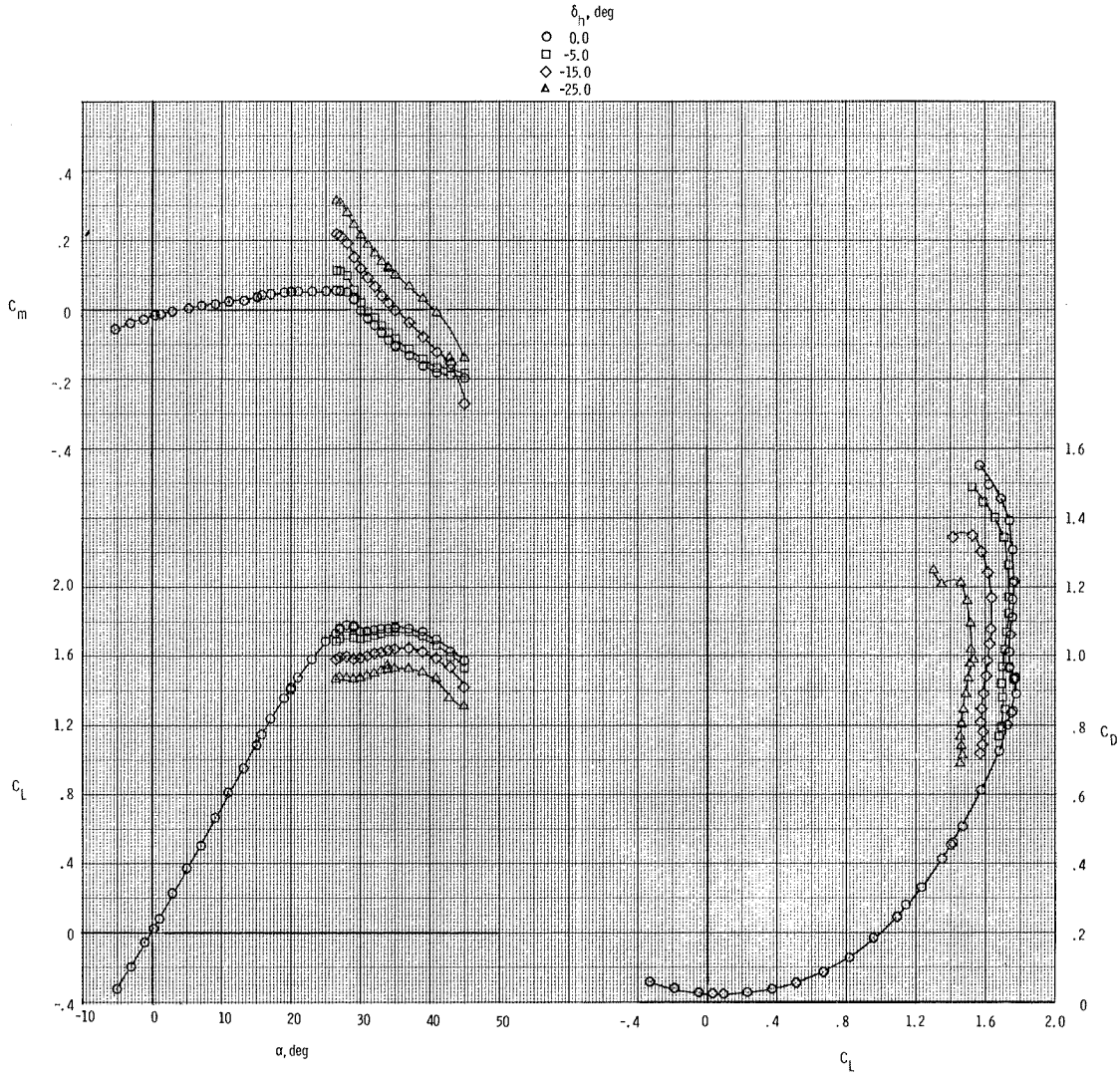

Figure 5.- Effect of horizontal tail deflection on the longitudinal aerodynamic characteristics with canard on. M = 0.40; Γ_c = 20°; δ_c = -9°.

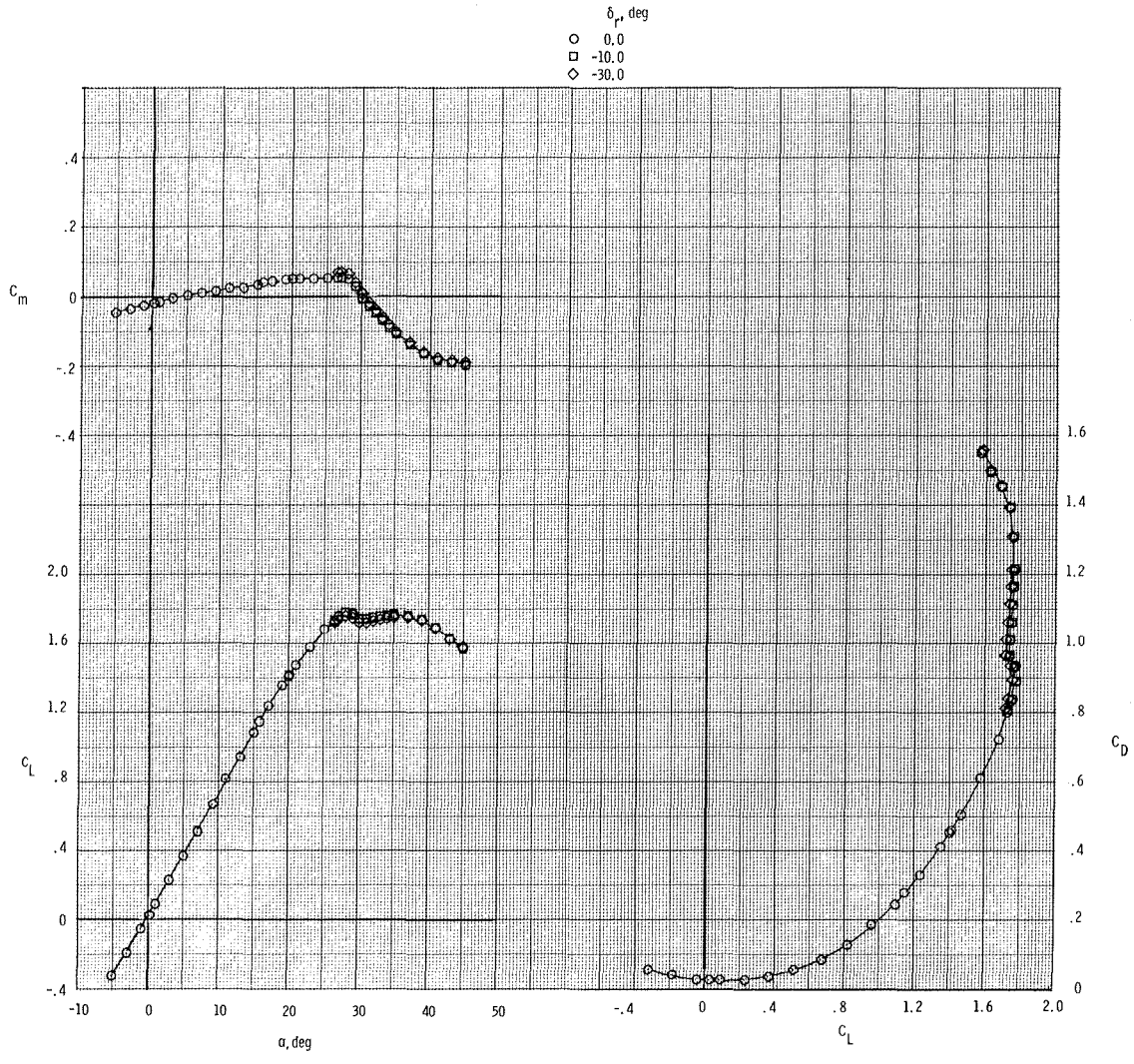

(a) Longitudinal characteristics.

Figure 6.- Effect of rudder deflection on the aerodynamic characteristics with canard on. M = 0.40; Γ_c = 20°; δ_c = -9°; δ_h = 0°.

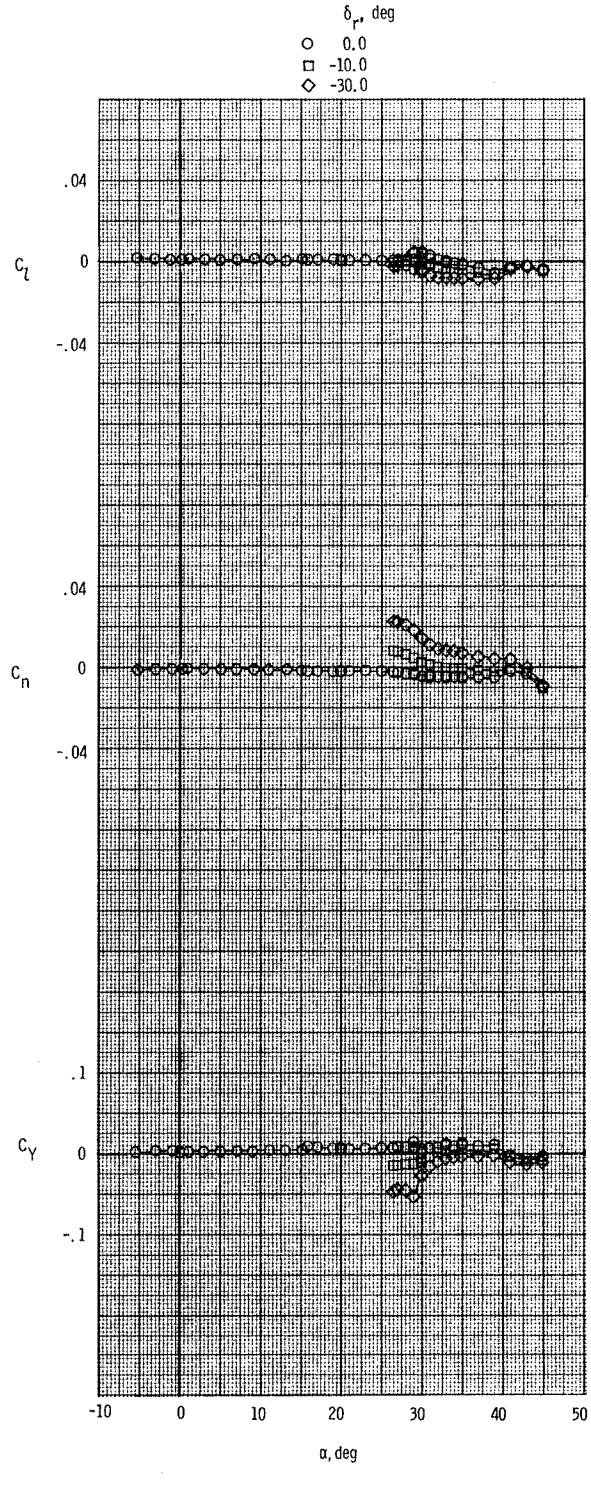

(b) Lateral-directional characteristics.

Figure 6.- Concluded.

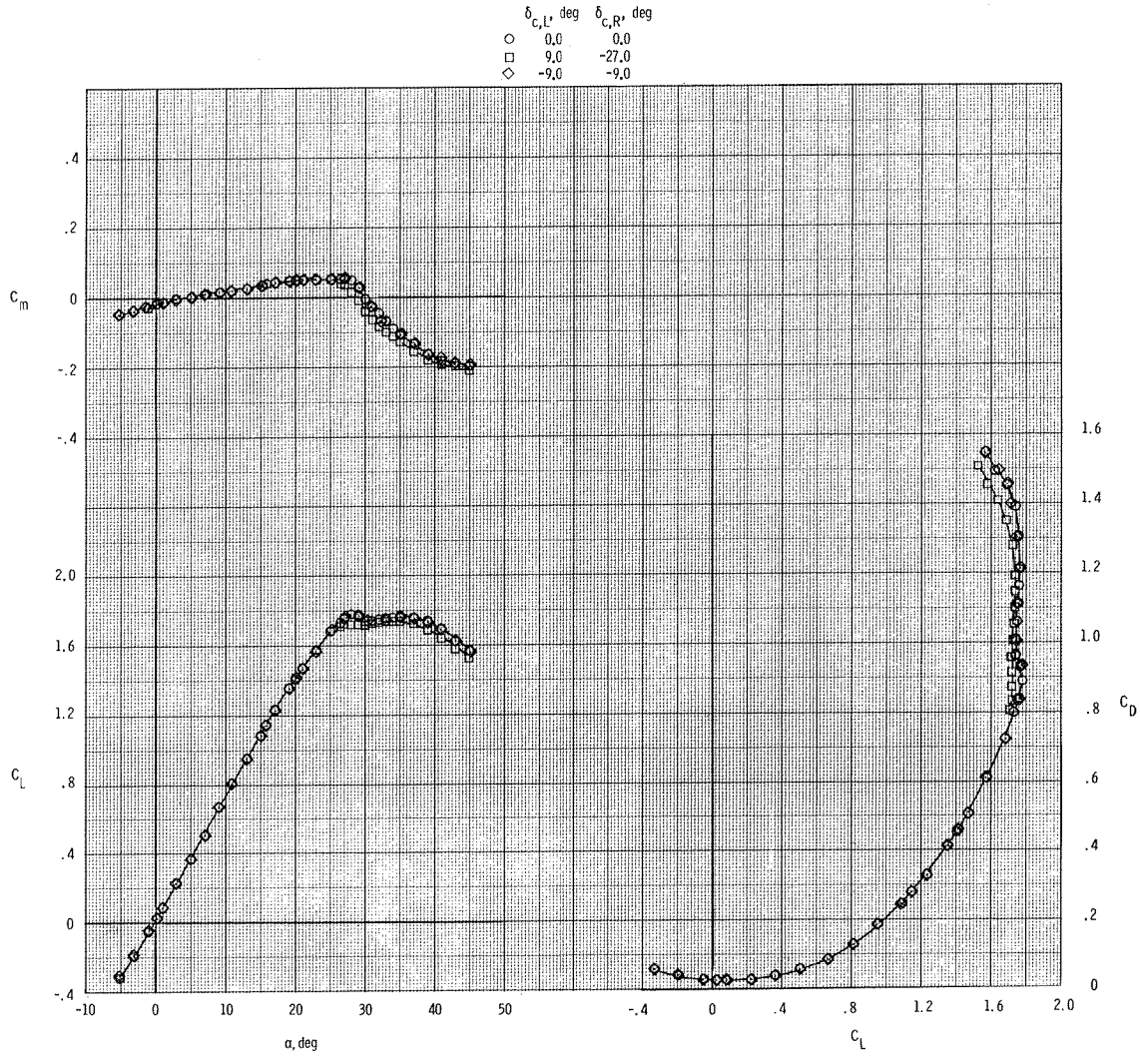

(a) Longitudinal characteristics.

Figure 7.- Effect of differential canard deflections on the aerodynamic characteristics. M = 0.40; Γ_c = 20°; δ_h = 0°.

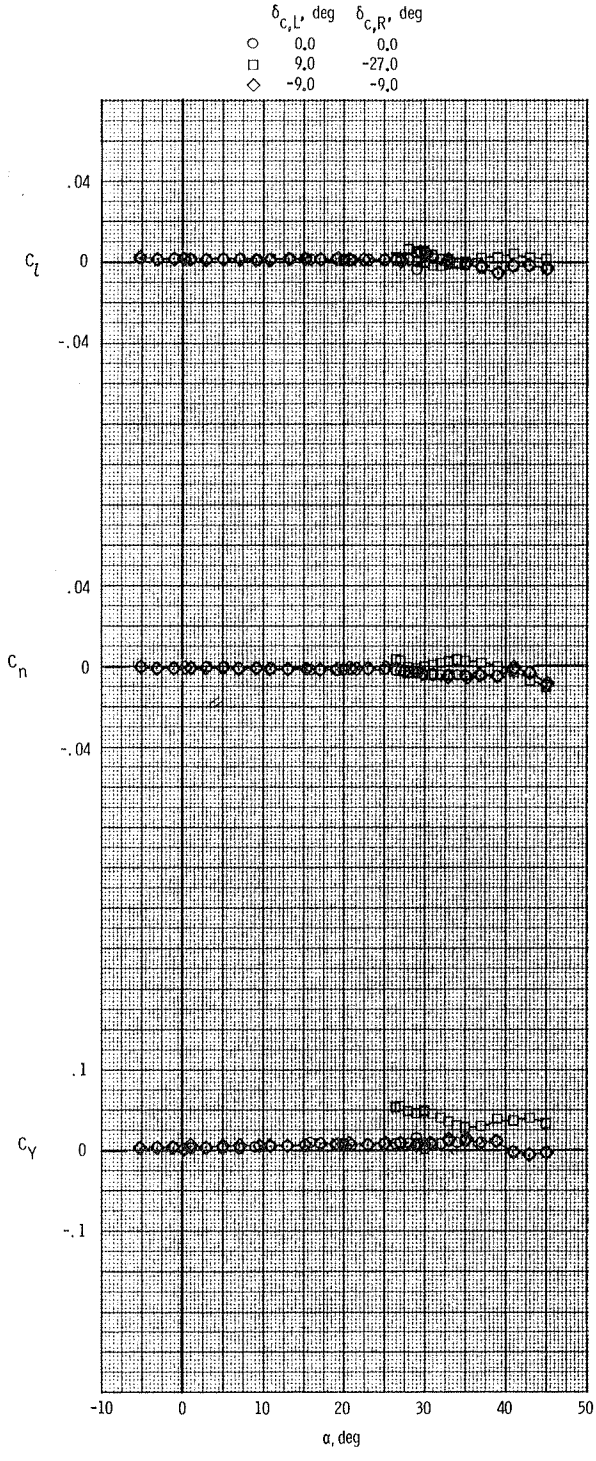

(b) Lateral-directional characteristics.

Figure 7.- Concluded.

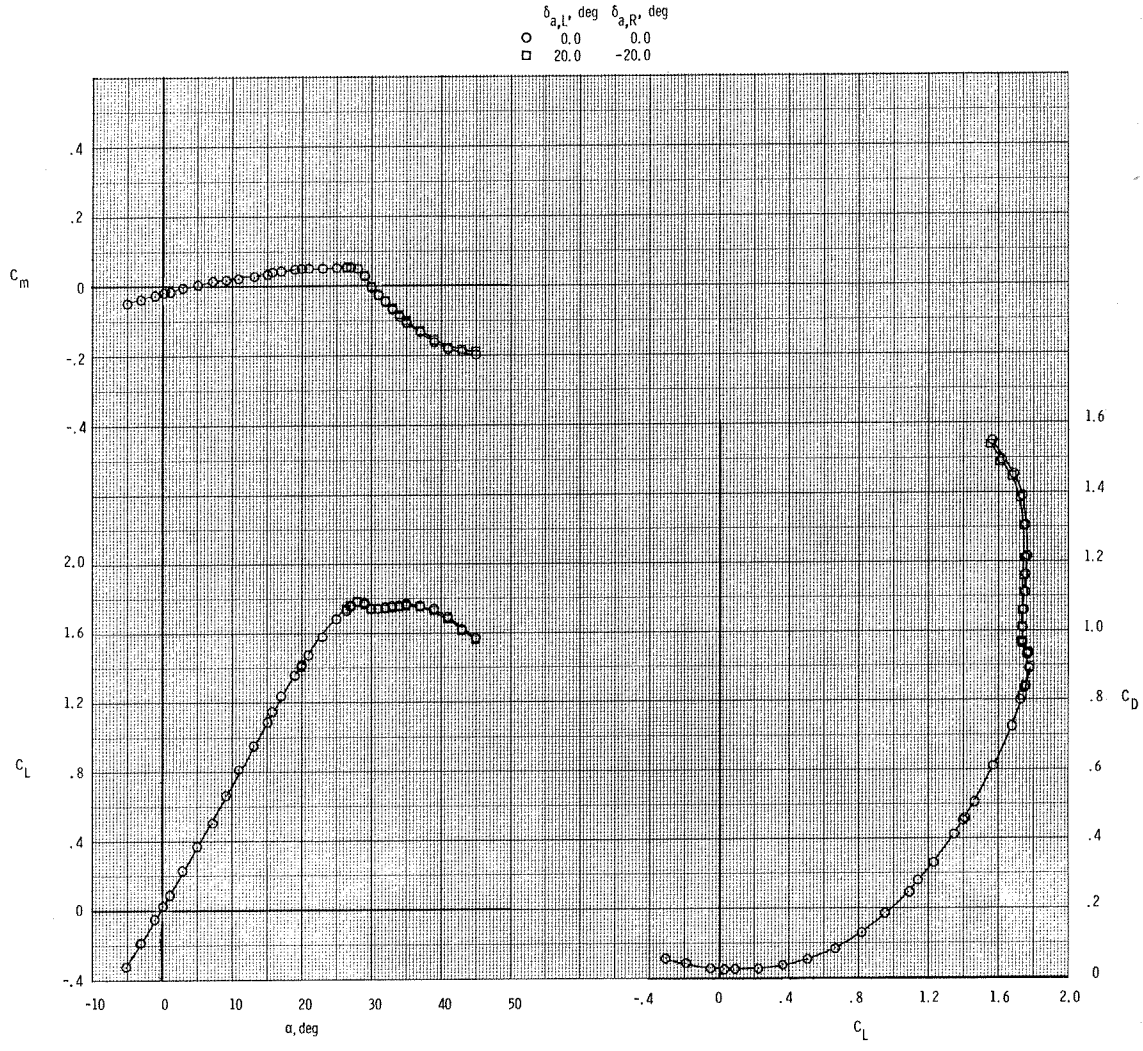

(a) Longitudinal characteristics.

Figure 8.- Effect of differential aileron deflections on the aerodynamic characteristics with canard on. M = 0.40; Γ_c = 20°; δ_c = -9°; δ_h = 0°.

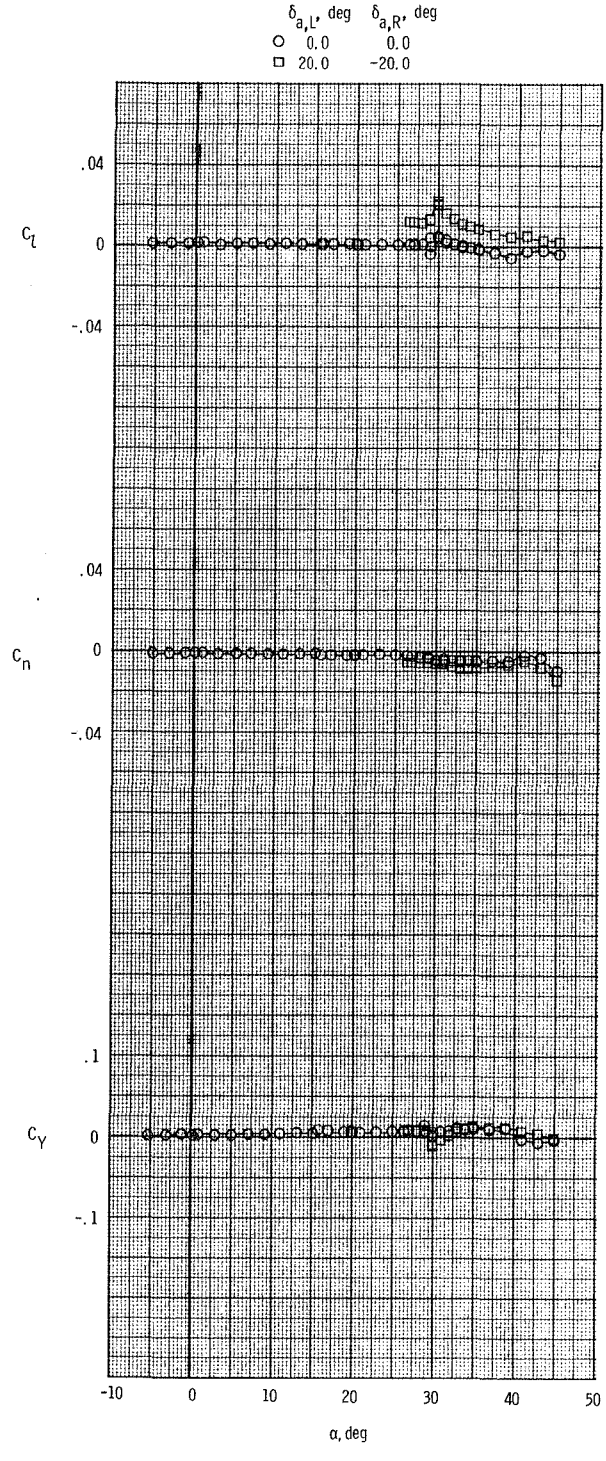

(b) Lateral-directional characteristics.

Figure 8.- Concluded.

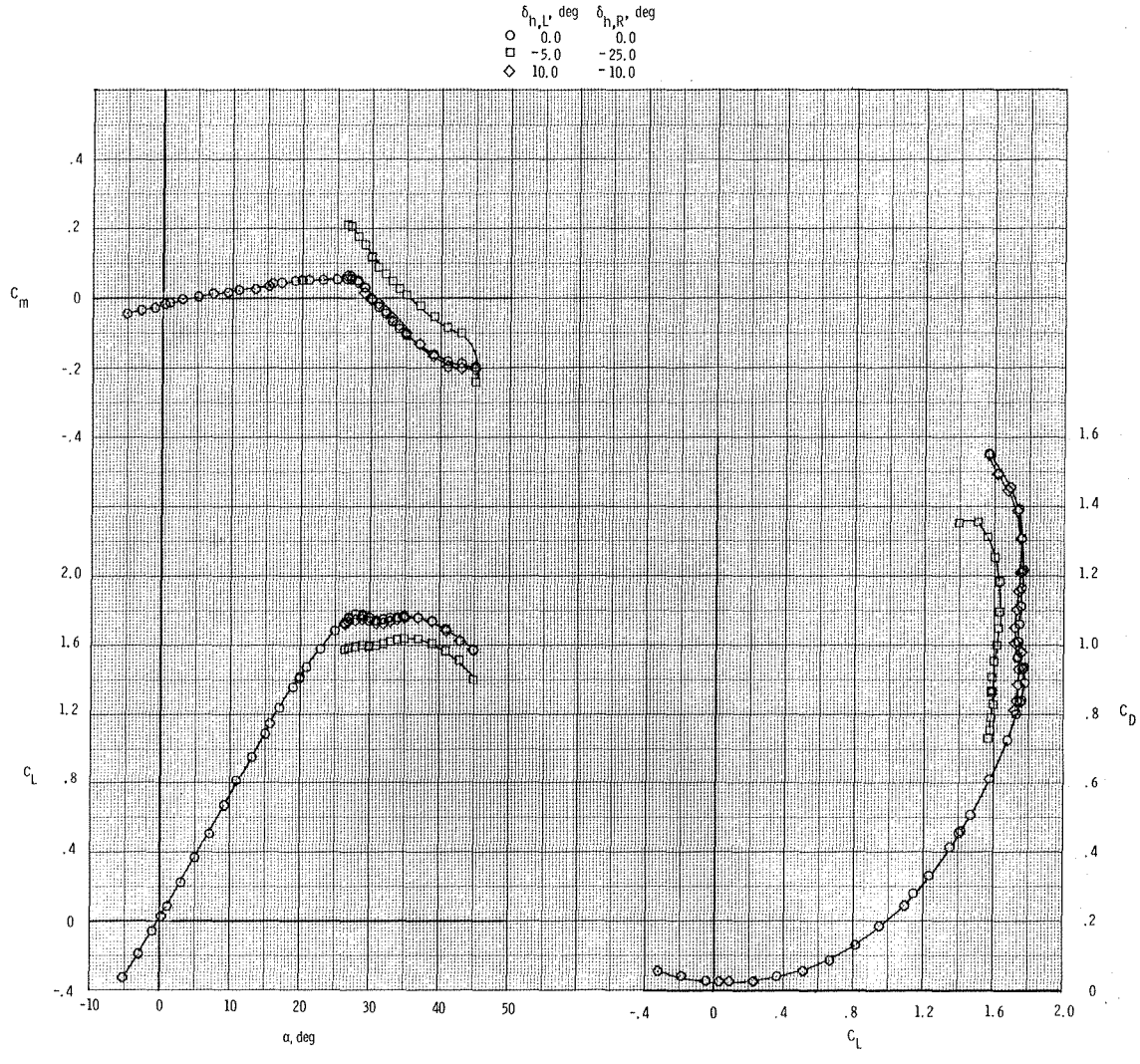

(a) Longitudinal characteristics.

Figure 9.- Effect of differential deflections of horizontal tails on the aerodynamic characteristics with canard on. M = 0.40; Γ_c = 20°; δ_c = -9°.

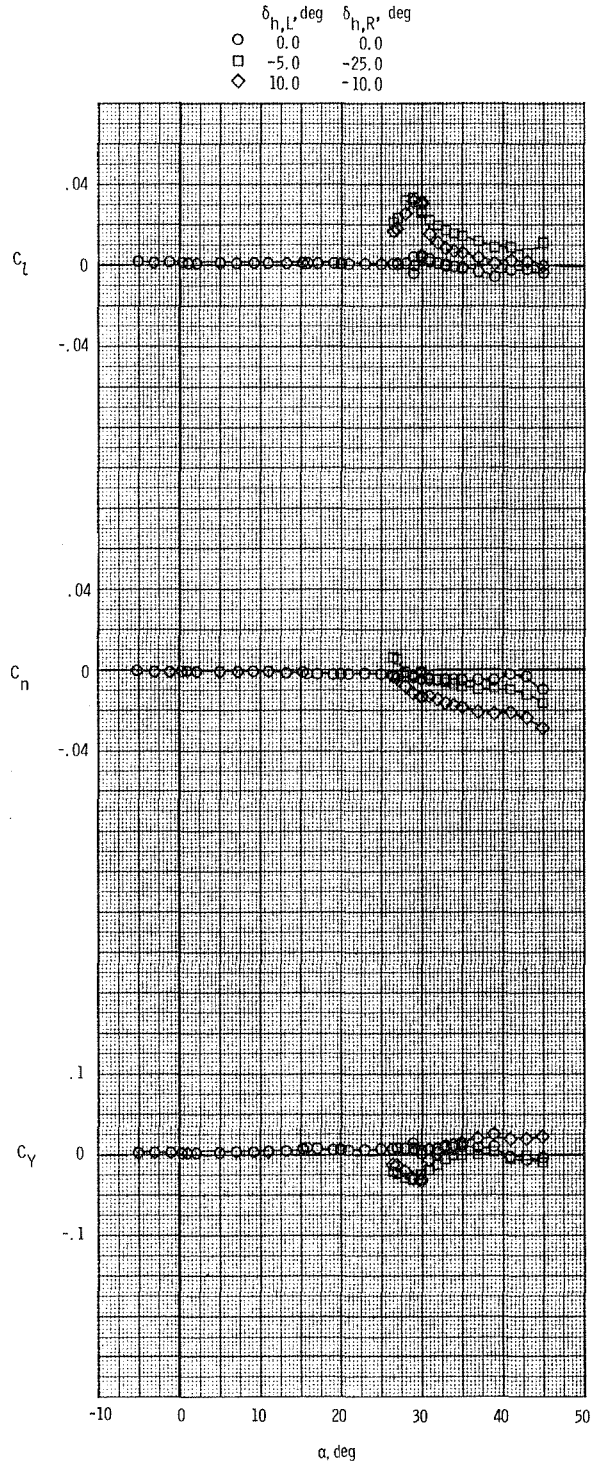

(b) Lateral-directional characteristics.

Figure 9.- Concluded.

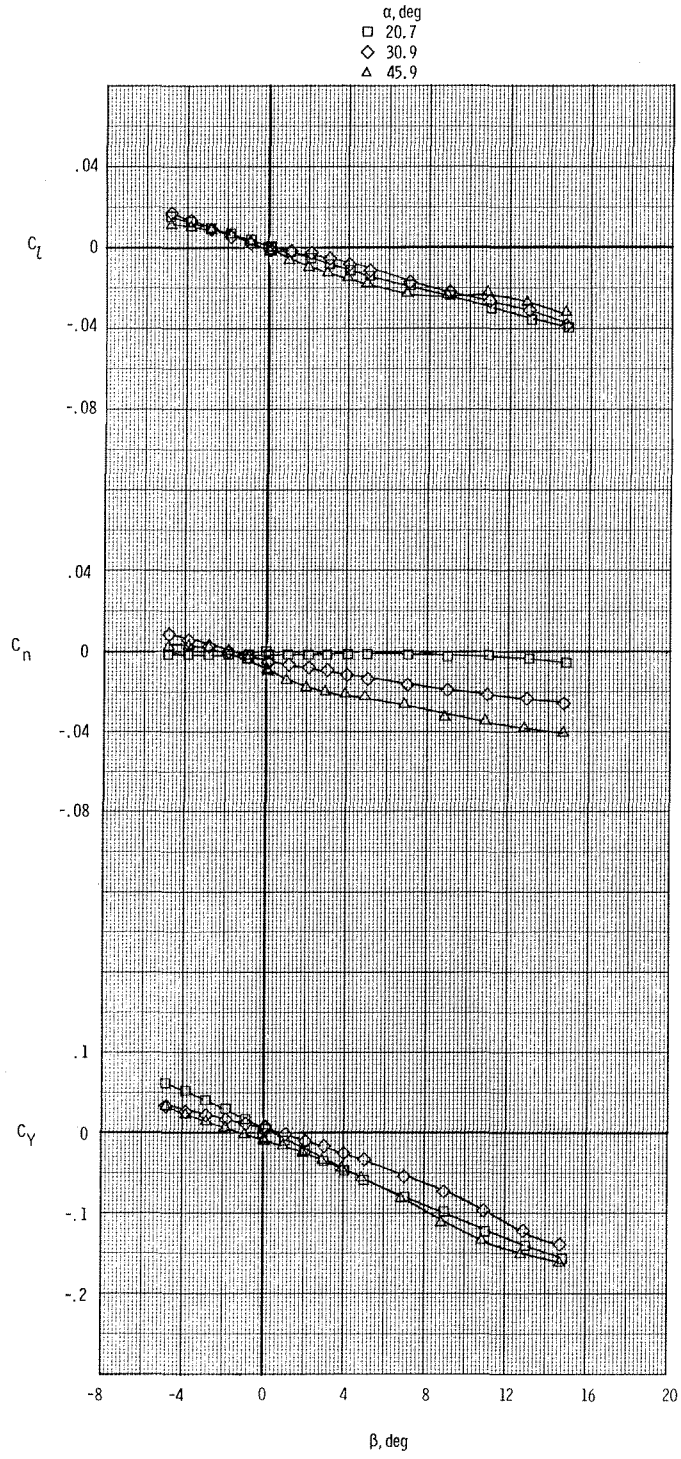

(a) M = 0.40.

Figure 10.- Effect of angle of attack on the lateral-directional characteristics without canard. $\delta_h = 0°$.

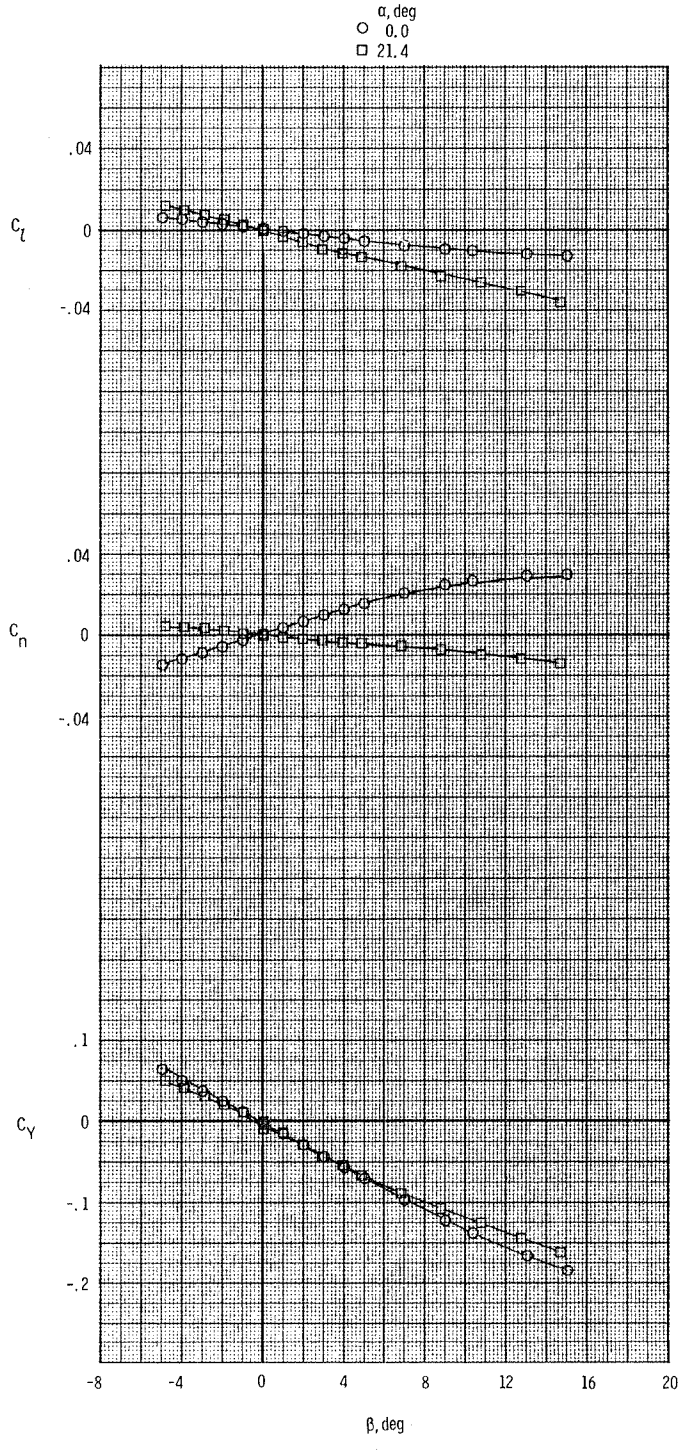

(b) M = 0.60.

Figure 10.- Continued.

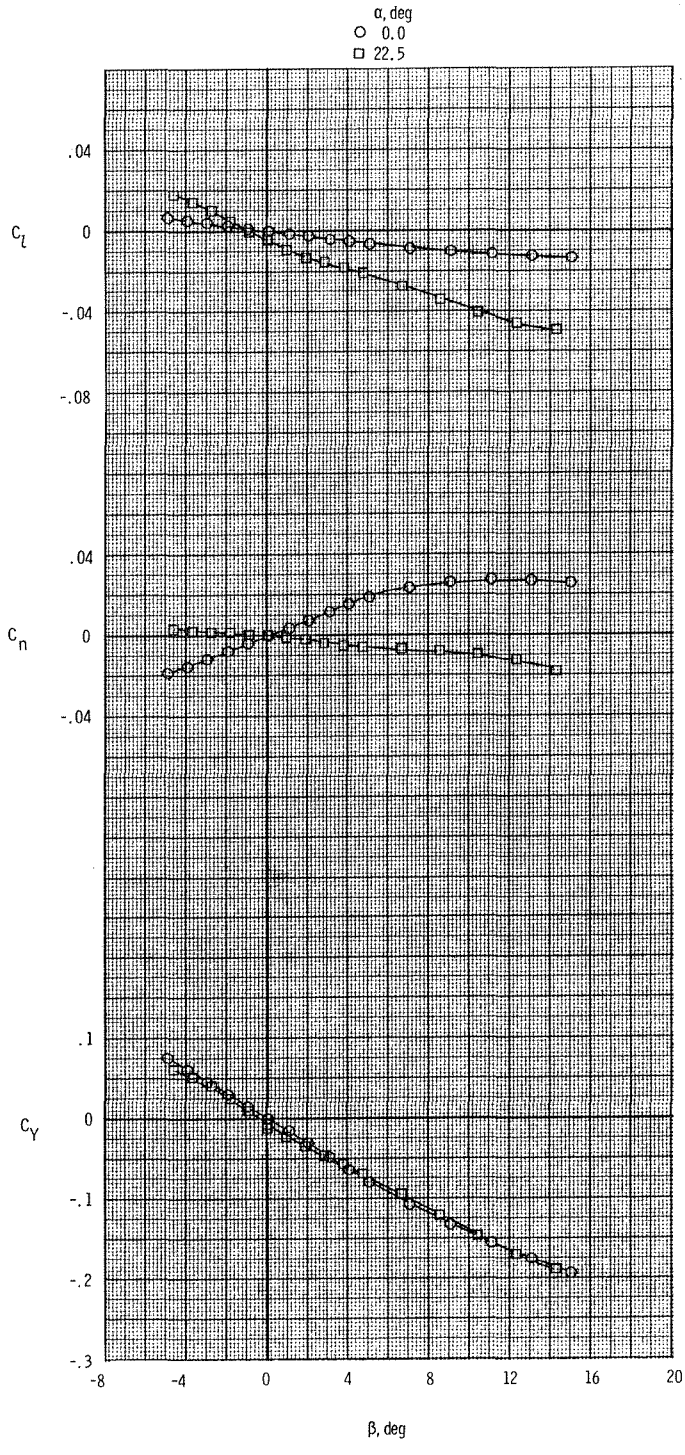

(c) M = 0.90.

Figure 10.- Concluded.

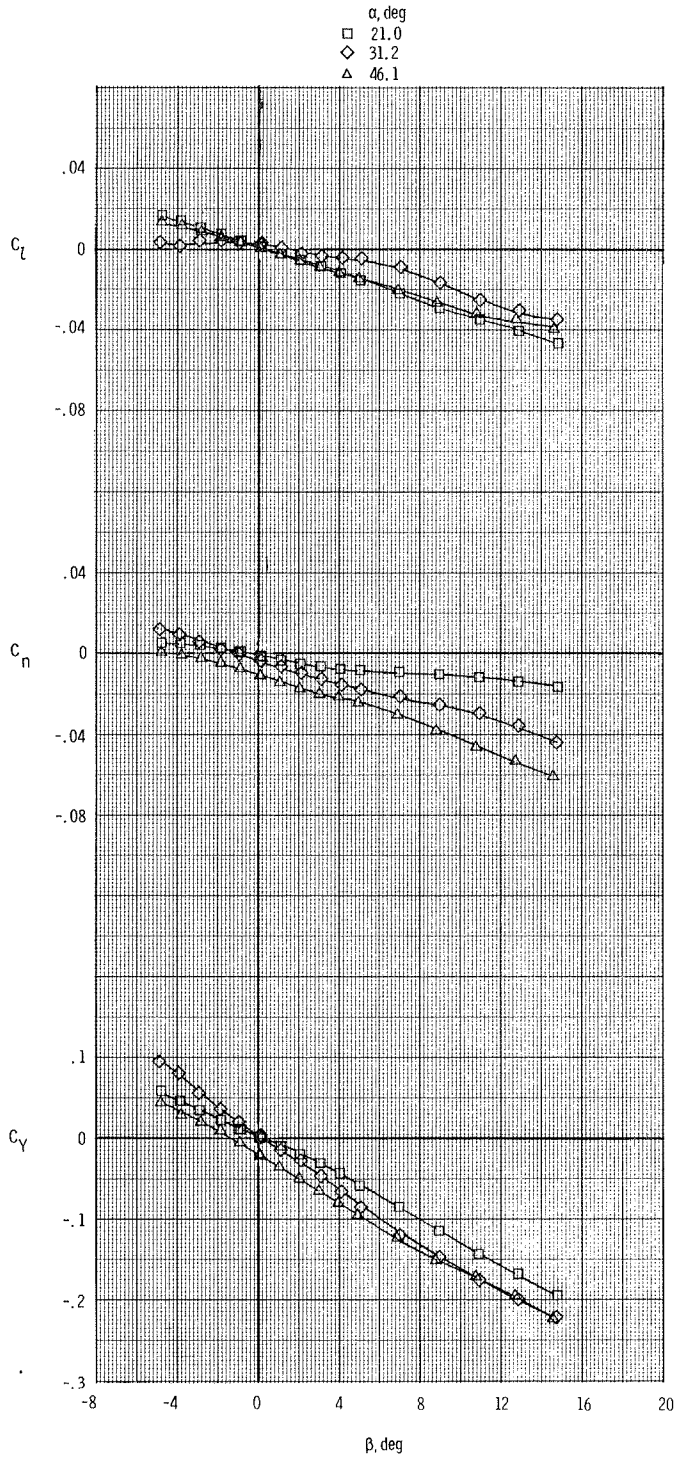

(a) M = 0.40.

Figure 11.- Effect of angle of attack on the lateral-directional characteristics with canard on and $\Gamma_c = 20°$. $\delta_c = -9°$; $\delta_h = 0°$.

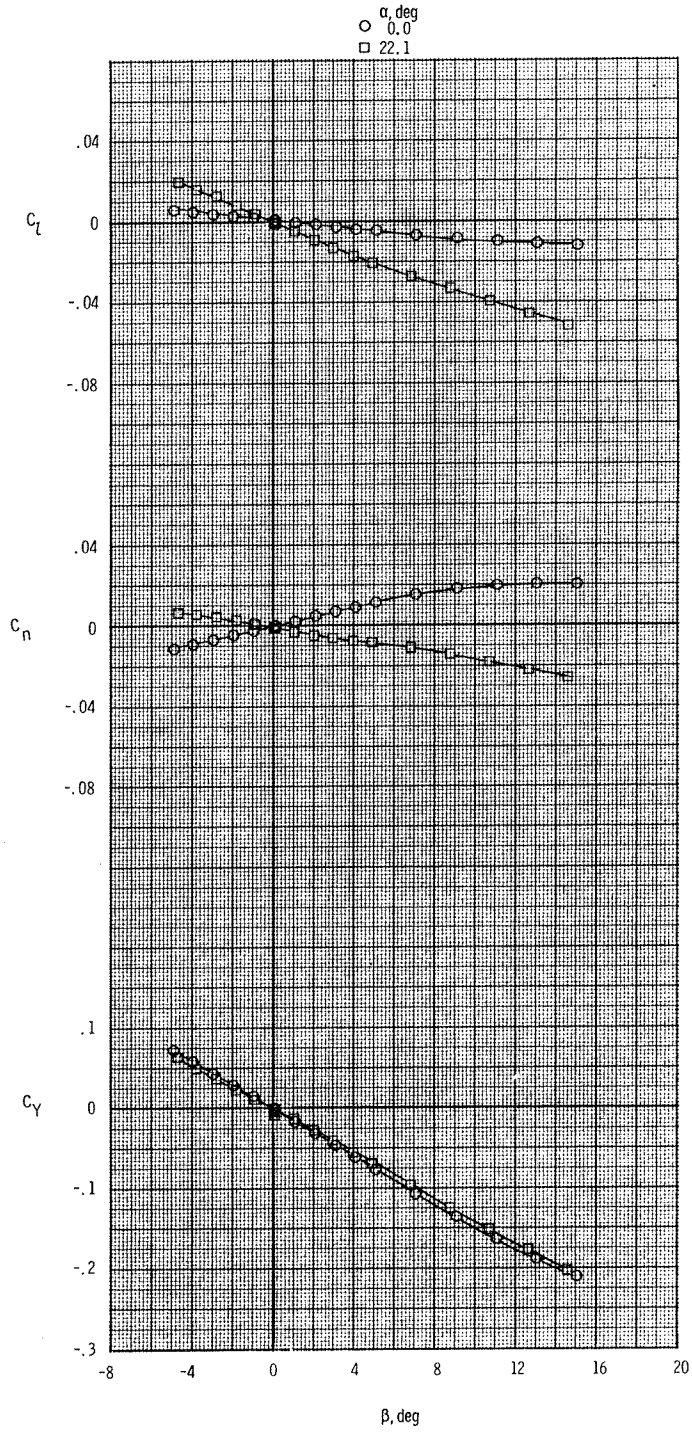

(b) M = 0.60.

Figure 11.- Continued.

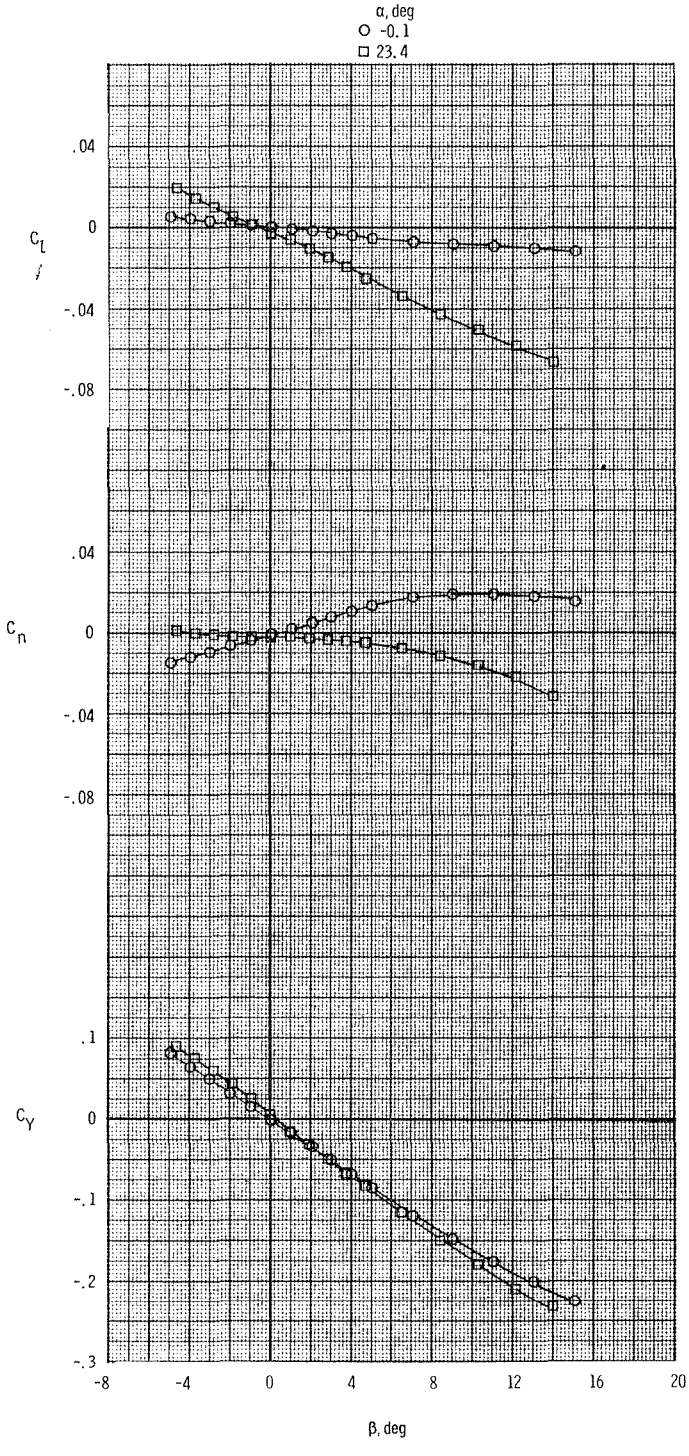

(c) M = 0.90.

Figure 11.- Concluded.

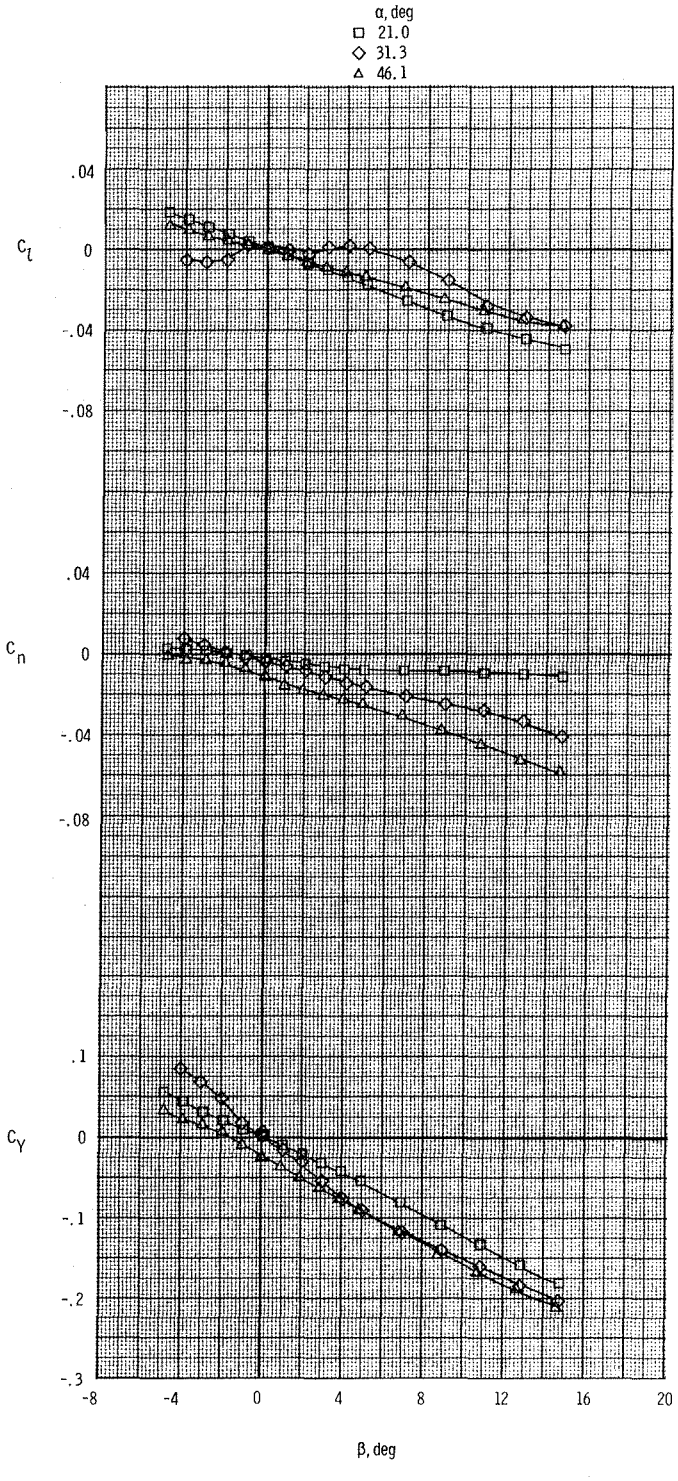

(a) M = 0.40.

Figure 12.- Effect of angle of attack on the lateral-directional characteristics with canard on and $\Gamma_c = 0°$. $\delta_c = -9°$; $\delta_h = 0°$.

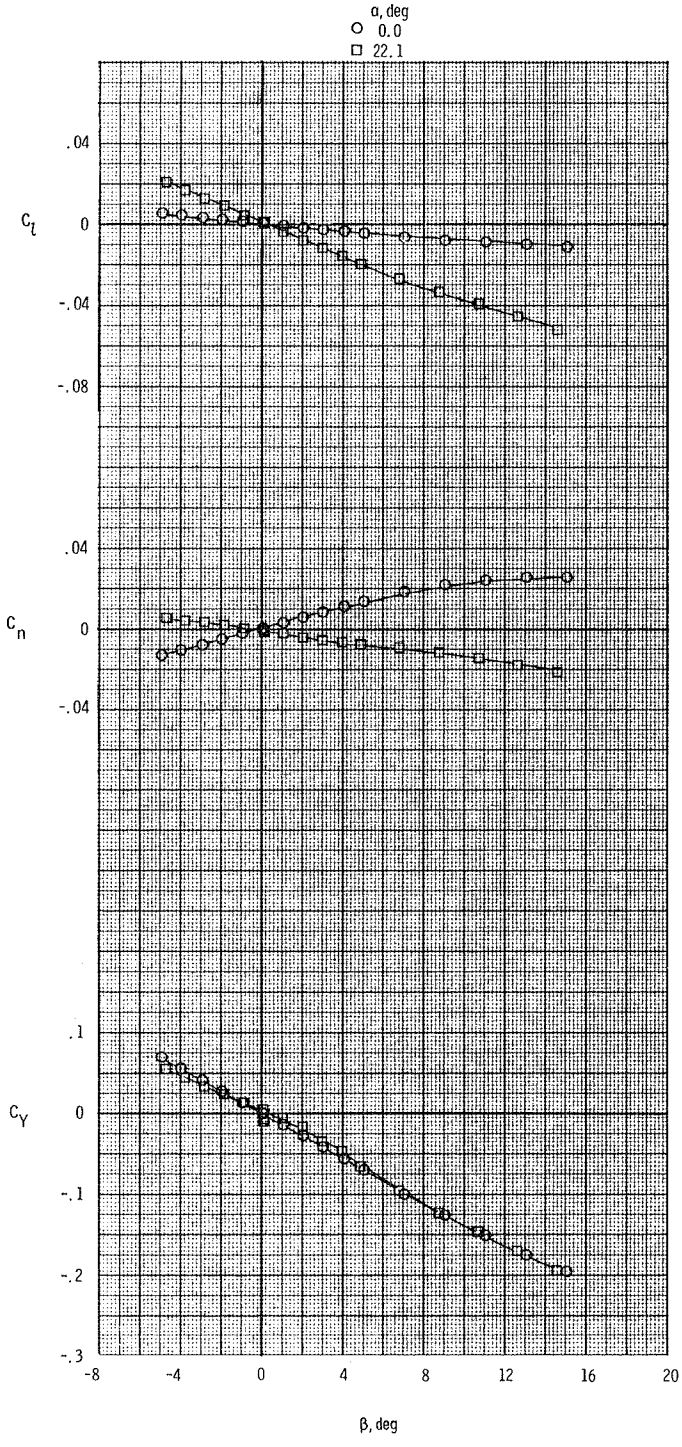

(b) M = 0.60.

Figure 12.- Continued.

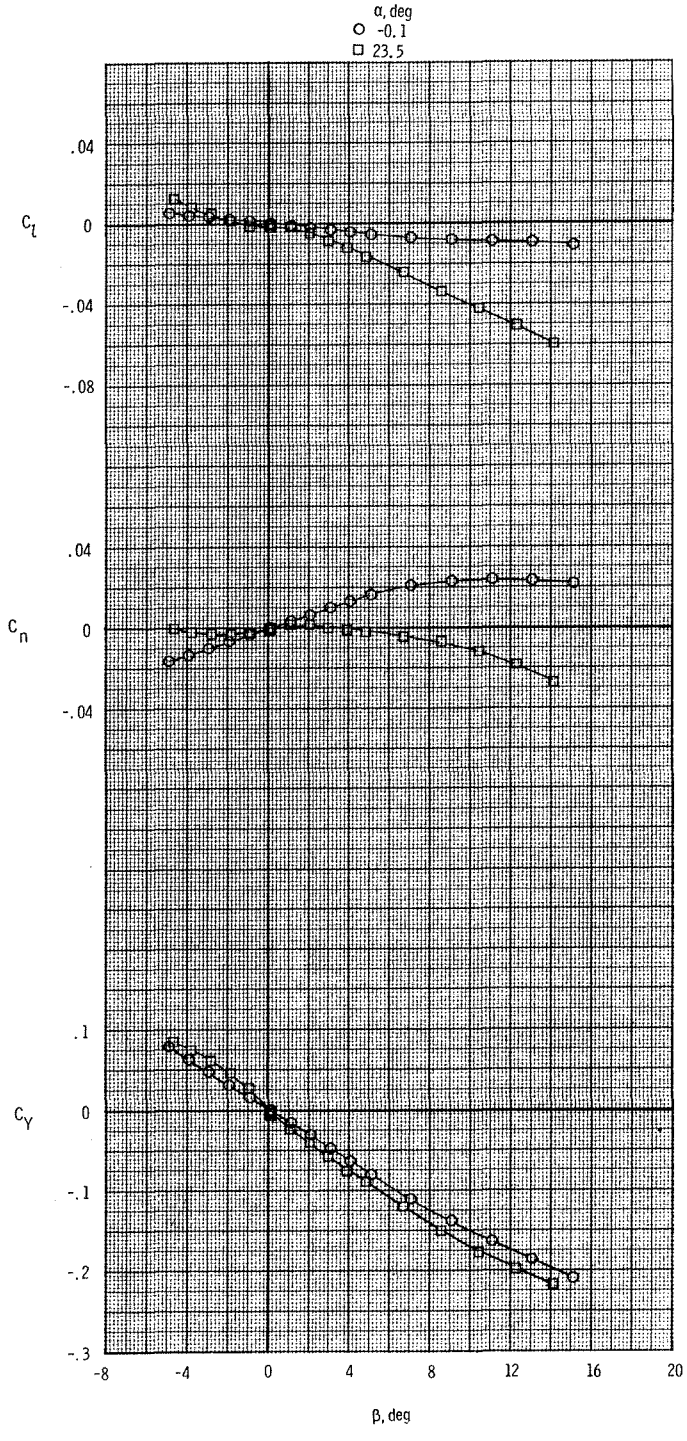

(c) M = 0.90.

Figure 12.- Concluded.

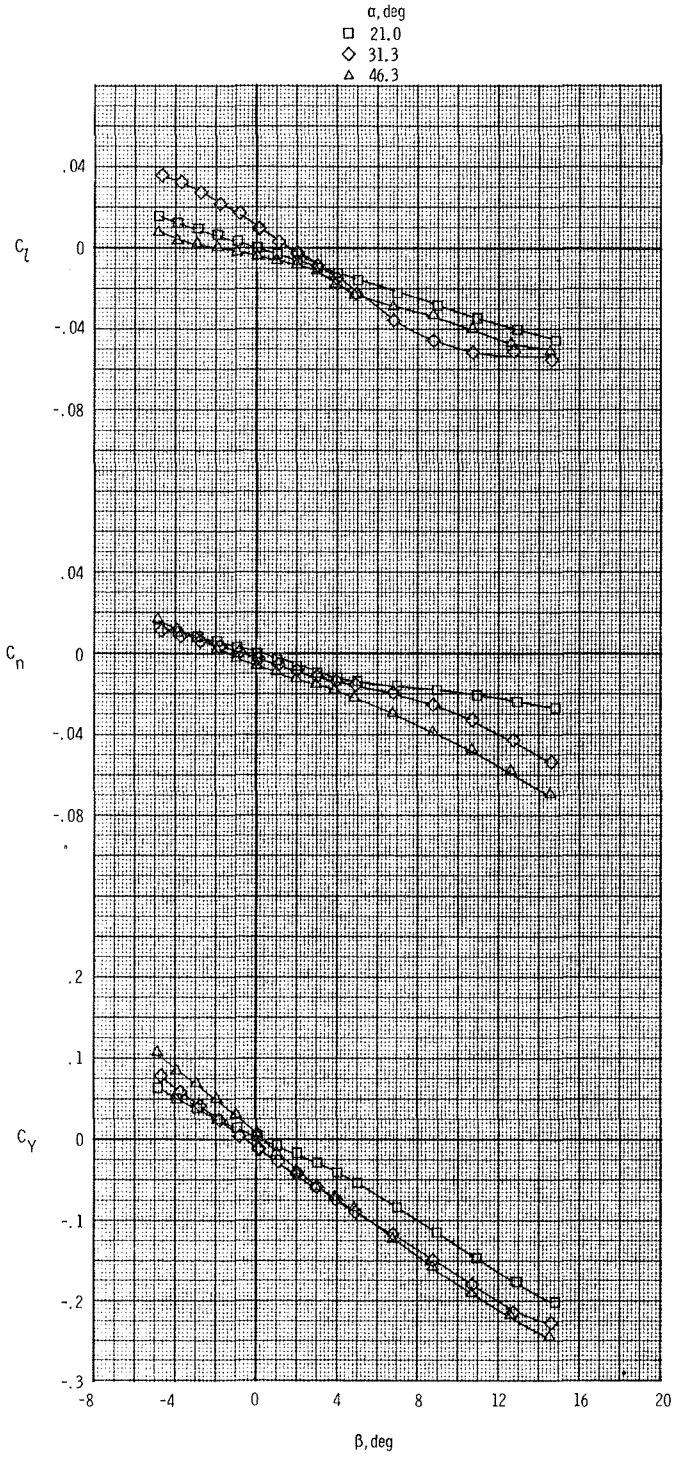

Figure 13.- Effect of angle of attack on the lateral-directional characteristics with the canard and strake on. $M = 0.40$; $\Gamma_c = 20°$; $\delta_c = -9°$; $\delta_h = 0°$.

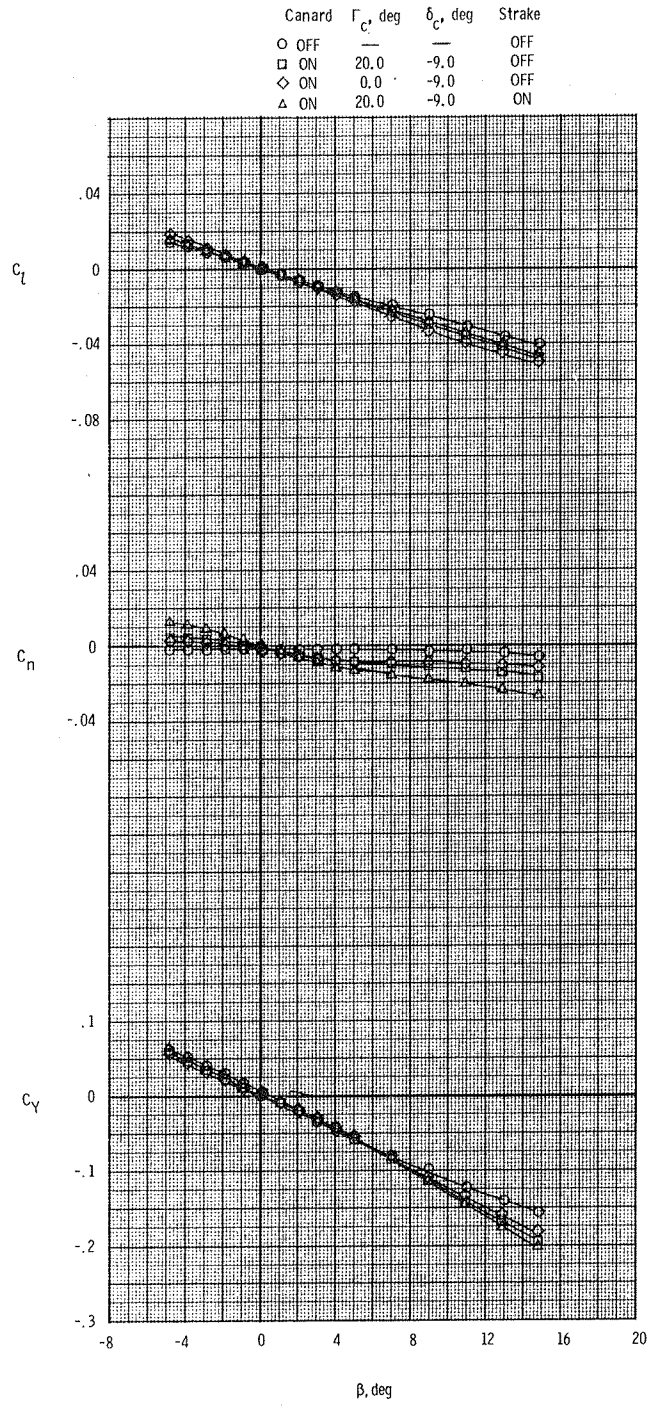

(a) $\alpha = 21°$.

Figure 14.- Effect of configuration variables on lateral-directional characteristics at $M = 0.40$. $\delta_h = 0°$.

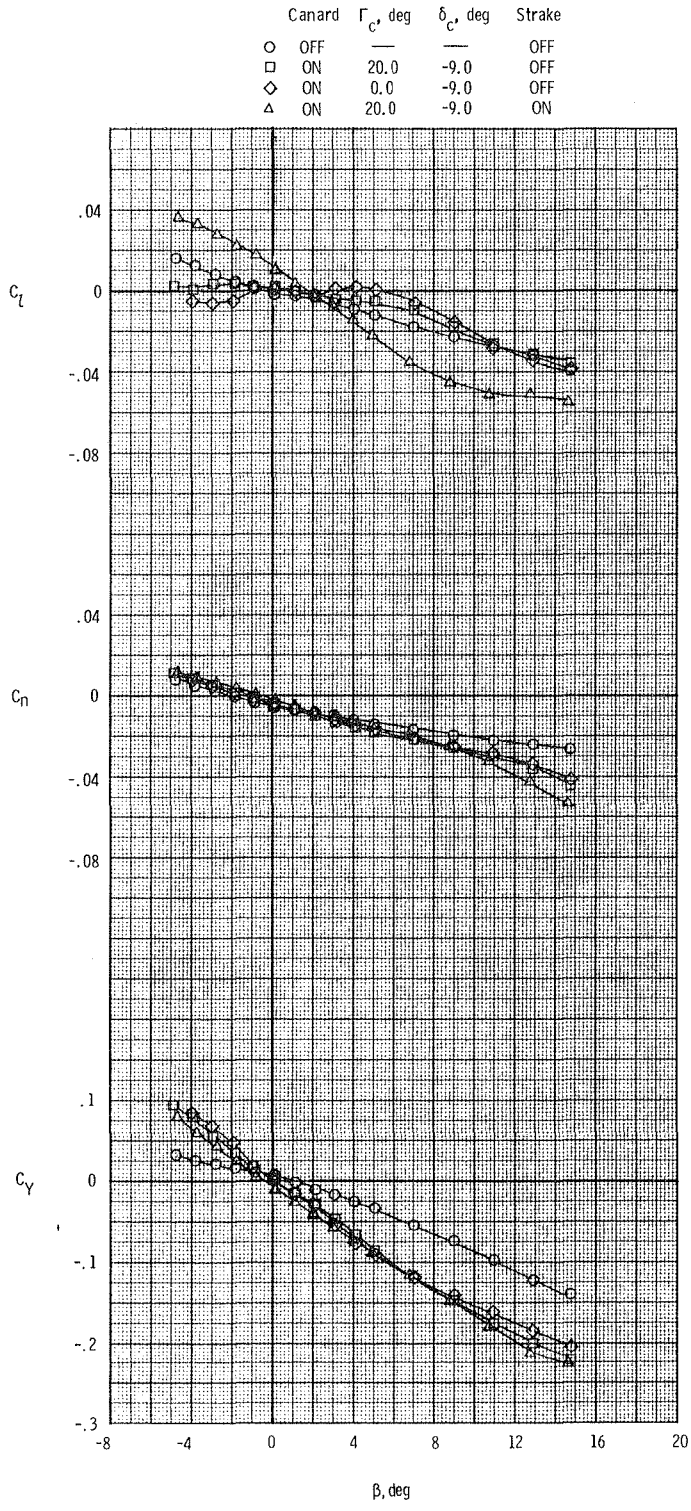

(b) $\alpha = 31°$.

Figure 14.- Continued.

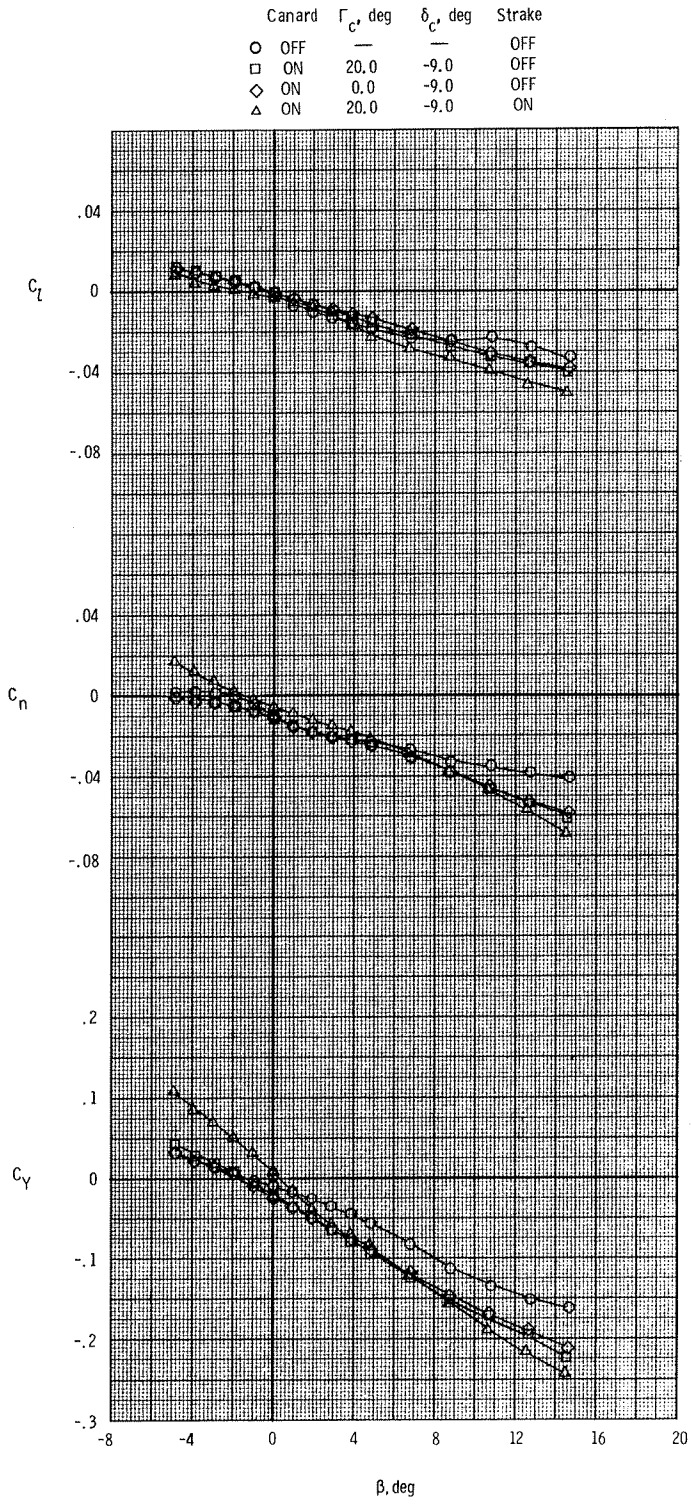

(c) $\alpha = 46°$.

Figure 14.- Concluded.

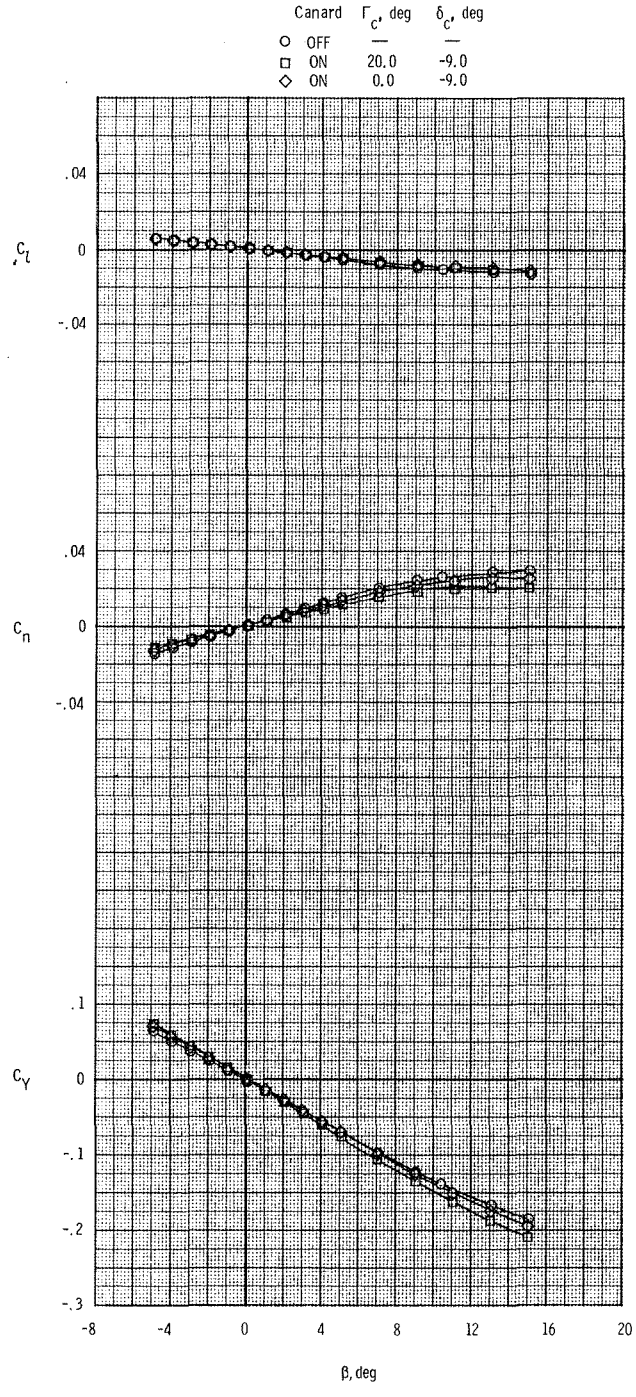

(a) $\alpha = 0°$.

Figure 15.- Effect of configuration variables on lateral-directional characteristics at $M = 0.60$. $\delta_h = 0°$.

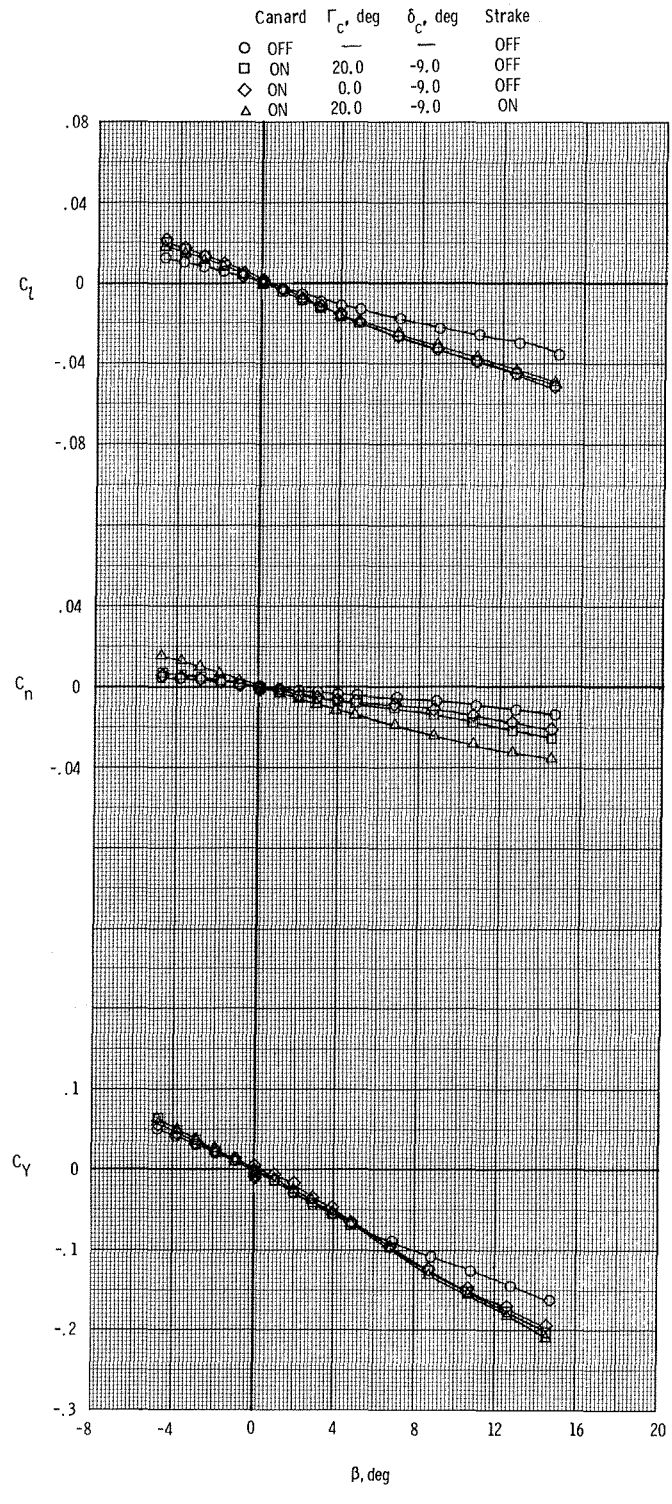

(b) $\alpha = 21°$.

Figure 15.- Concluded.

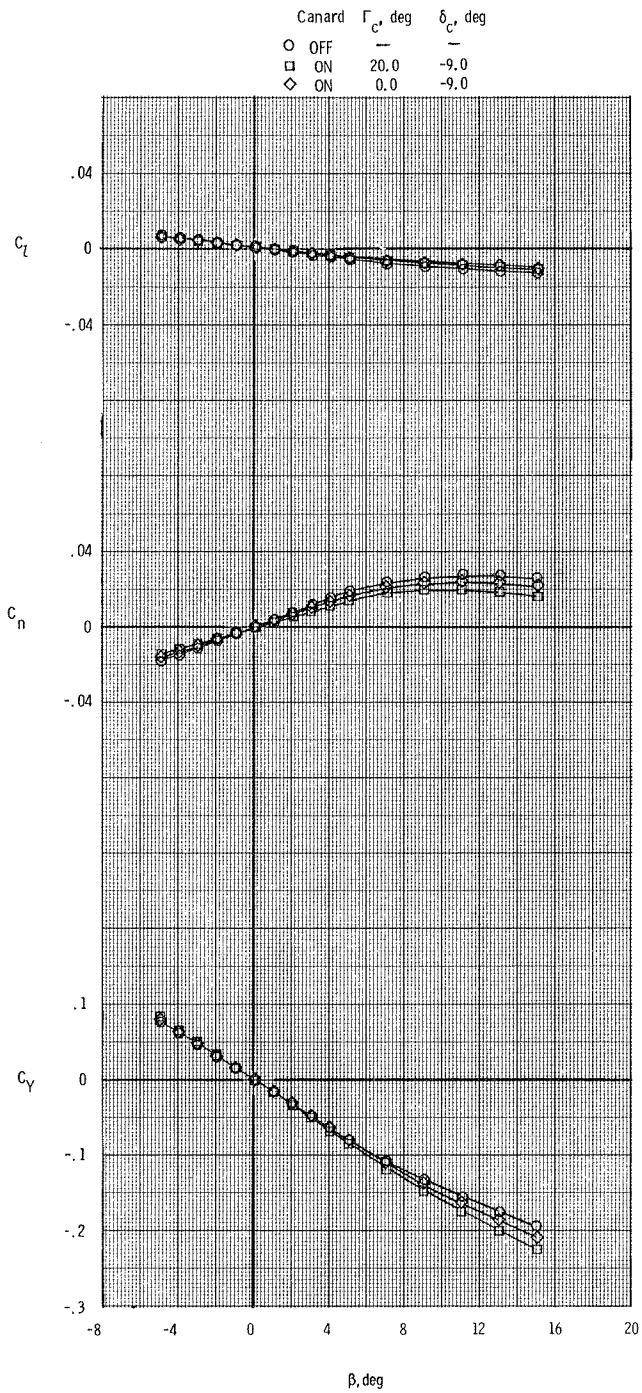

(a) $\alpha = 0°$.

Figure 16.- Effect of configuration variables on lateral-directional characteristics at $M = 0.90$. $\delta_h = 0°$.

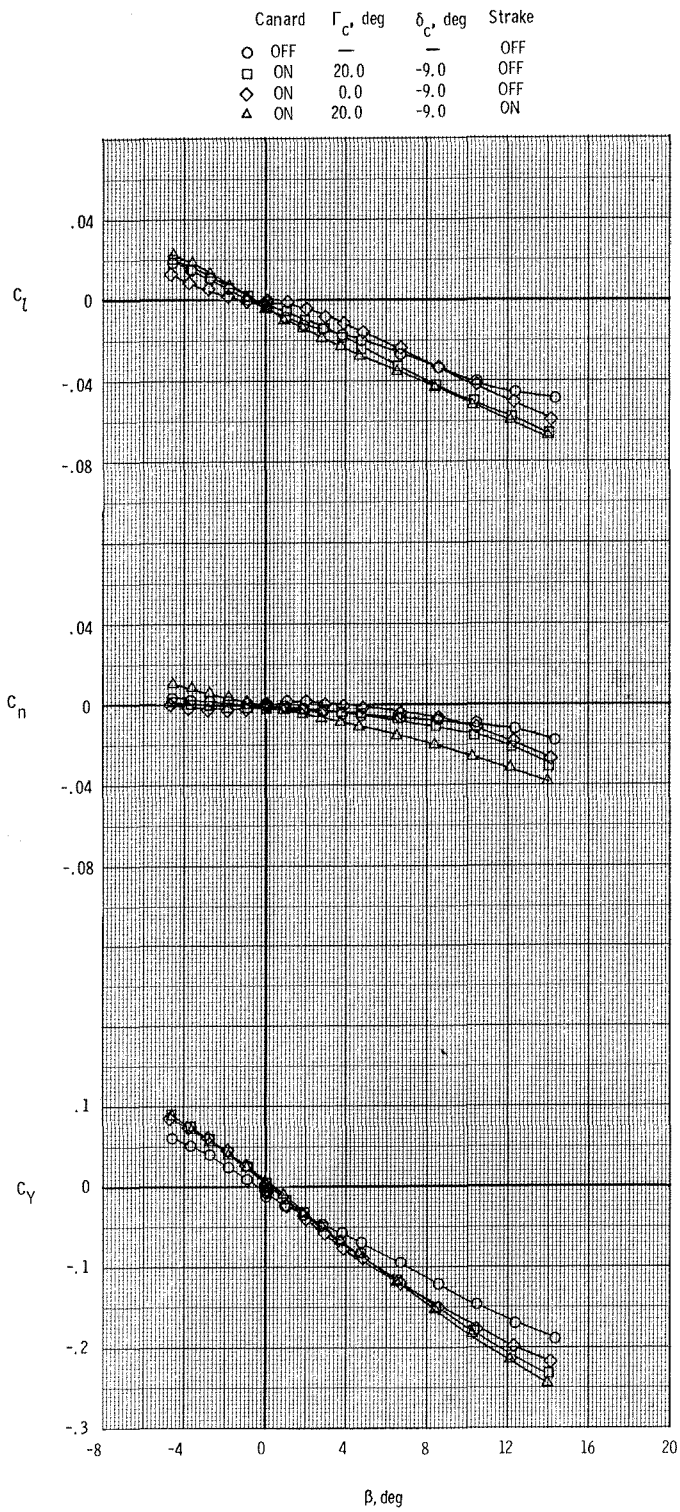

(b) $\alpha = 23°$.

Figure 16.- Concluded.

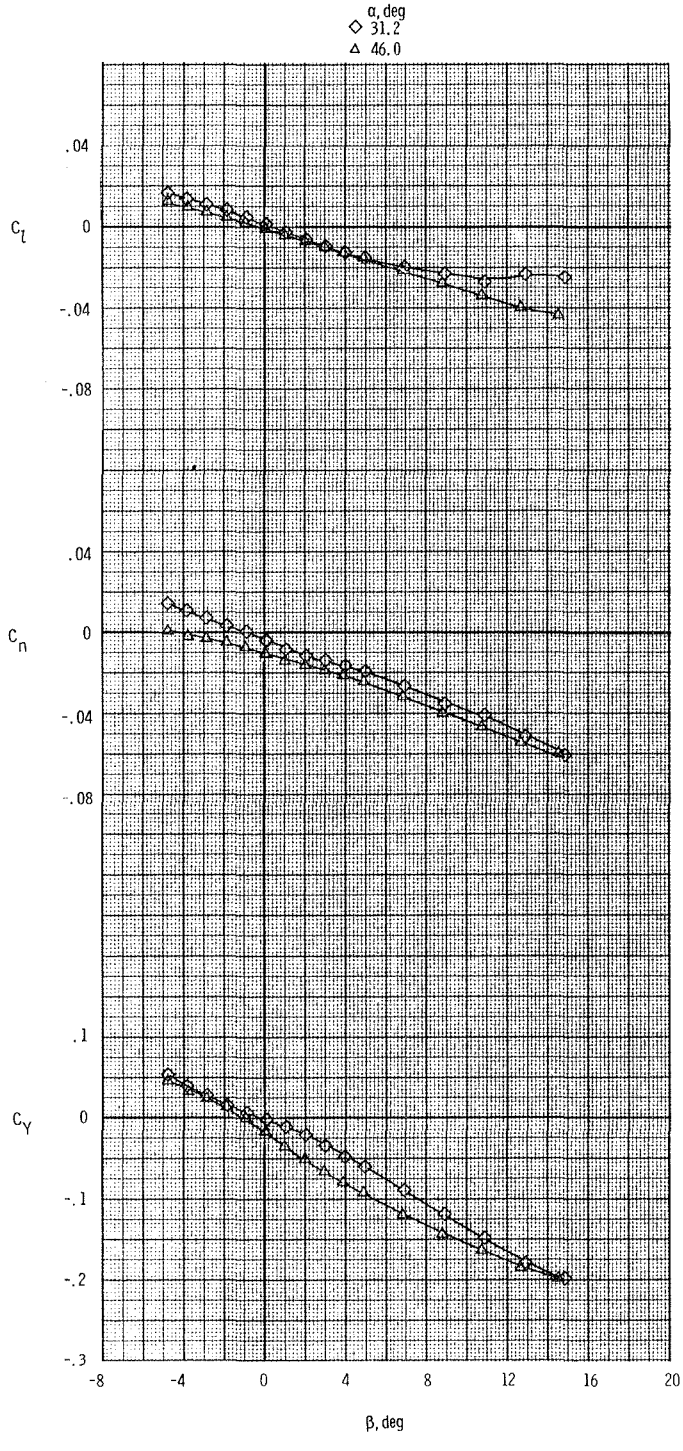

(a) $\delta_c = -9.0°$.

Figure 17.- Effect of angle of attack on lateral-directional characteristics with canard on. M = 0.40; $\Gamma_c = 20°$; $\delta_h = -25°$.

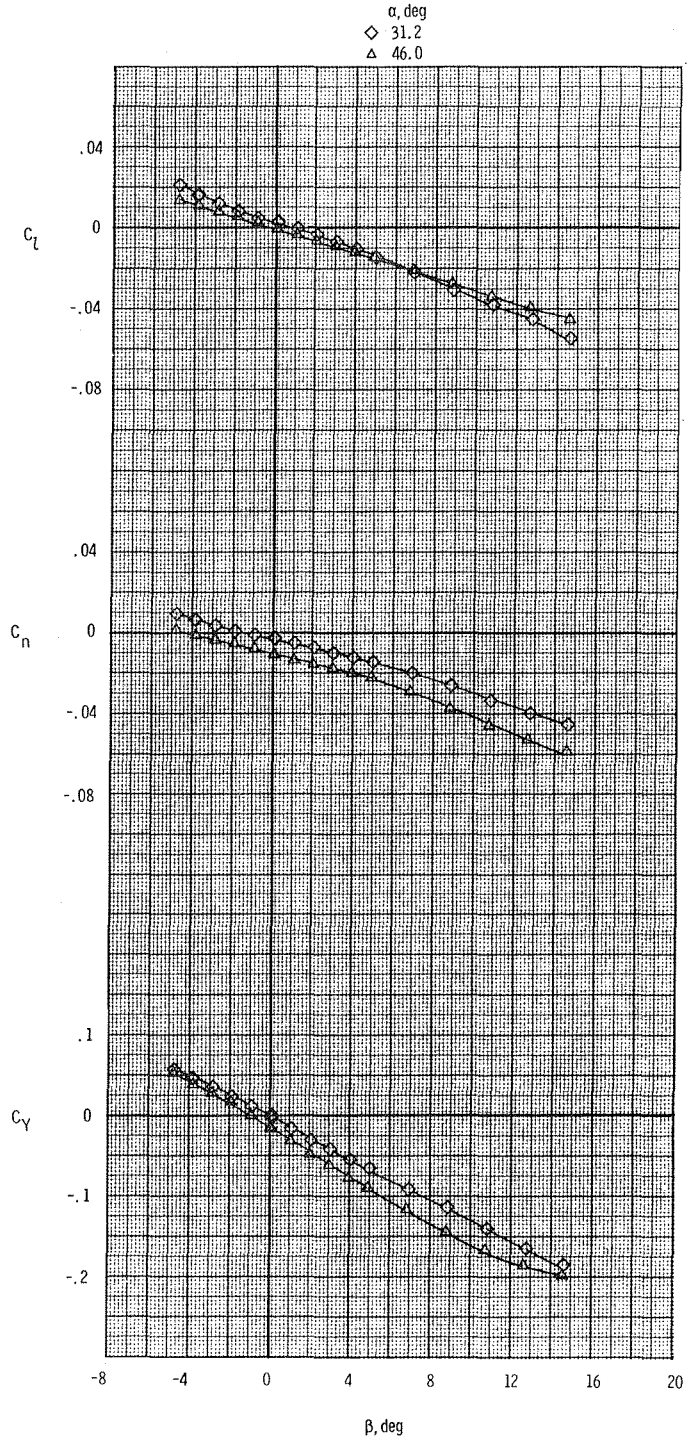

(b) $\delta_c = -27.0°$.

Figure 17.- Concluded.

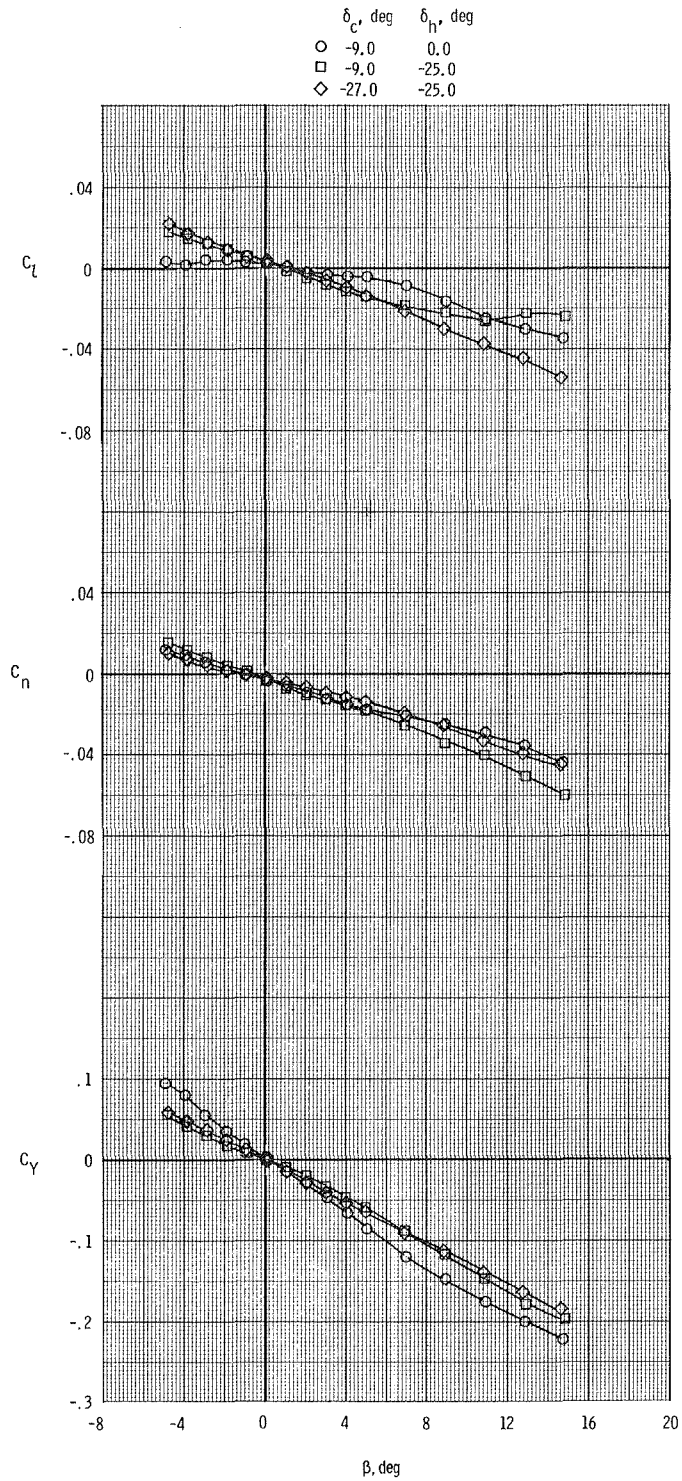

(a) $\alpha = 31.2°$.

Figure 18.- Effect of deflections of canard and horizontal tails on lateral-directional characteristics. $M = 0.40$; $\Gamma_c = 20°$.

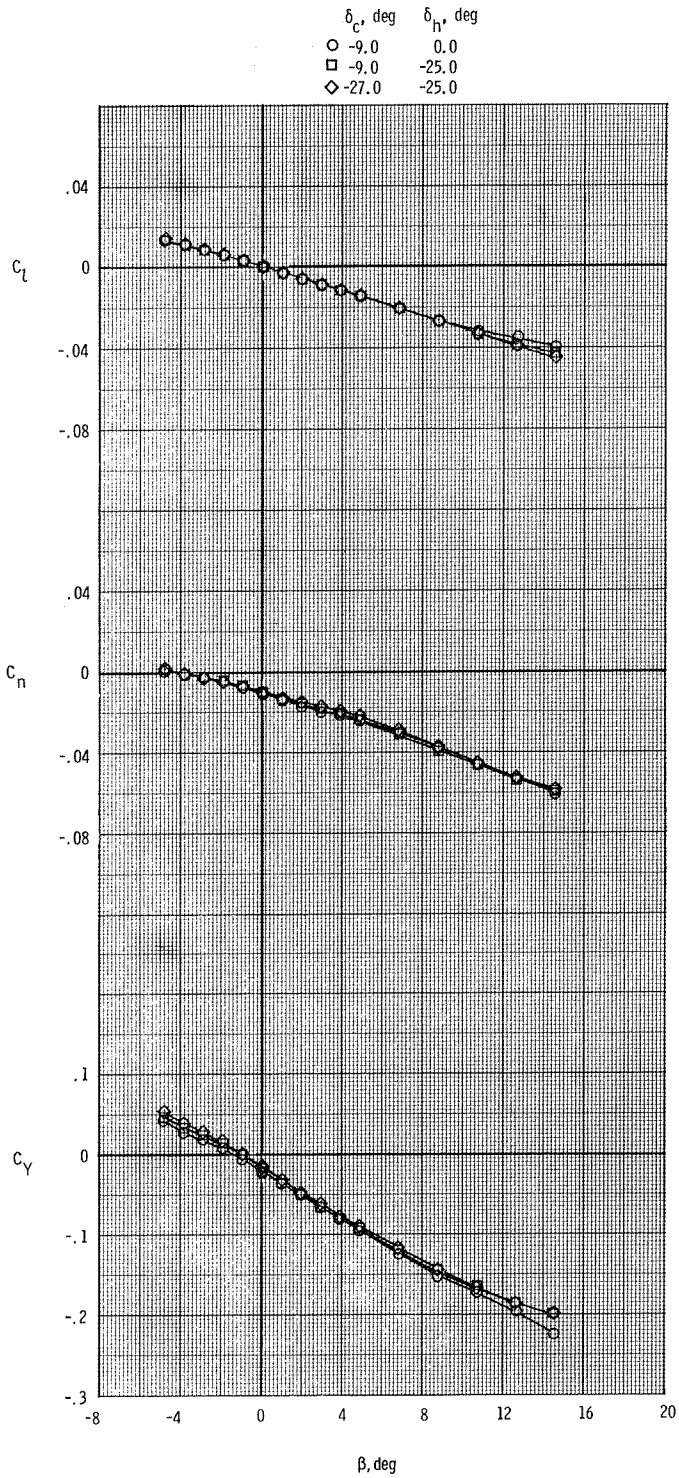

(b) $\alpha = 46.1°$.

Figure 18.- Concluded.

1. Report No.	2. Government Accession No.	3. Recipient's Catalog No.
NASA TM-83171		

4. Title and Subtitle	5. Report Date
STABILITY AND CONTROL CHARACTERISTICS OF A THREE-SURFACE ADVANCED FIGHTER CONFIGURATION AT ANGLES OF ATTACK UP TO 45°	September 1981
	6. Performing Organization Code: 505-43-23-01

7. Author(s)	8. Performing Organization Report No.
William P. Henderson and Laurence D. Leavitt	L-14433
	10. Work Unit No.

9. Performing Organization Name and Address	11. Contract or Grant No.
NASA Langley Research Center Hampton, VA 23665	
	13. Type of Report and Period Covered: Technical Memorandum

12. Sponsoring Agency Name and Address	14. Sponsoring Agency Code
National Aeronautics and Space Administration Washington, DC 20546	

15. Supplementary Notes

16. Abstract

An investigation has been conducted to determine the stability and control characteristics of a three-surface (canard-wing-horizontal-tail) advanced fighter configuration. The tests were conducted at Mach numbers from 0.40 to 0.90, at angles of attack up to 45° for the lower Mach numbers, and at angles of sideslip up to 15°. The model variations under study included adding a canard surface and deflecting horizontal tails, ailerons, and rudders.

17. Key Words (Suggested by Author(s))	18. Distribution Statement
Aerodynamics Stability and control Fighter aircraft	Unclassified - Unlimited Subject Category 02

19. Security Classif. (of this report)	20. Security Classif. (of this page)	21. No. of Pages	22. Price
Unclassified	Unclassified	45	A03

For sale by the National Technical Information Service, Springfield, Virginia 22161

NASA-Langley, 1981

End of Document